united nations
educational, scientific
and cultural
organization

international atomic
energy agency

the
abdus salam
international centre for theoretical physics

40th anniversary 1964 2004

H4.SMR/1586-20

"7th Workshop on Three-Dimensional Modelling
of Seismic Waves Generation and their Propagation"

25 October - 5 November 2004

Global Dynamics of the Earth
Applications of Normal Mode Relaxation Theory to Solid-Earth Geophysics

Roberto SABADINI
University of Milan
Department of Earth Sciences "A Desio"
Section of Geophysics
Milan, Italy

GLOBAL DYNAMICS OF THE EARTH
Applications of Normal Mode Relaxation Theory to Solid-Earth Geophysics

ROBERTO SABADINI
Section of Geophysics,
Department of Earth Sciences "A. Desio", University of Milan,
Via L. Cicognara 7, I-20129 Milano, Italy

BERT VERMEERSEN
Delft Institute for Earth-Oriented Space Research,
Faculty of Aerospace Engineering, Delft University of Technology,
Kluyverweg 1, NL-2629 HS Delft, The Netherlands

Kluwer Academic Publishers
Boston/Dordrecht/London

Chapter 1

NORMAL MODE THEORY IN VISCOELASTICITY

1. RHEOLOGICAL MODELS

In modeling a particular geophysical phenomenon, the choice of the rheology used depends on 1) mathematical difficulty, 2) the quality of the geophysical data which the calculations of the model are required to match and 3) our knowledge of the rheological behavior of the medium at hand. Over the last few decades a considerable amount of knowledge has been gained about mantle rheology in terms of the values of rheological parameters and deformation mechanisms. For instance, what is most important, as far as mantle convection is concerned, is clearly the strong temperature dependence of the viscosity which the laboratory-derived values of the activation energy and volume seem to suggest. This intense interest in understanding convection in a fluid with markedly temperature-dependent viscosity is attested by the recent fundamental studies by geophysicists using analytical, numerical and experimental methods. In what follows, however, rather than discussing topics of mantle rheology and mantle convection, for which we refer to the book by Ranalli (1995), we will try to address the main questions that are at issue in attempting to study transient and long time scale geodynamic phenomena in a wide arc of time scales, ranging from years, characteristic of post-seismic deformation, to hundreds of millions of years as in the case of true polar wander driven by subduction, making use of the analytical normal mode theory in viscoelasticity with different models of mantle rheology. In Figure 1.1 we sketch the entire geodynamic spectrum spanning the whole range of phenomenological time scales. One of the key questions is whether one can devise a constitutive law which can satisfactorily model all these phenomena, from the anelastic transient regime to the steady-state domain.

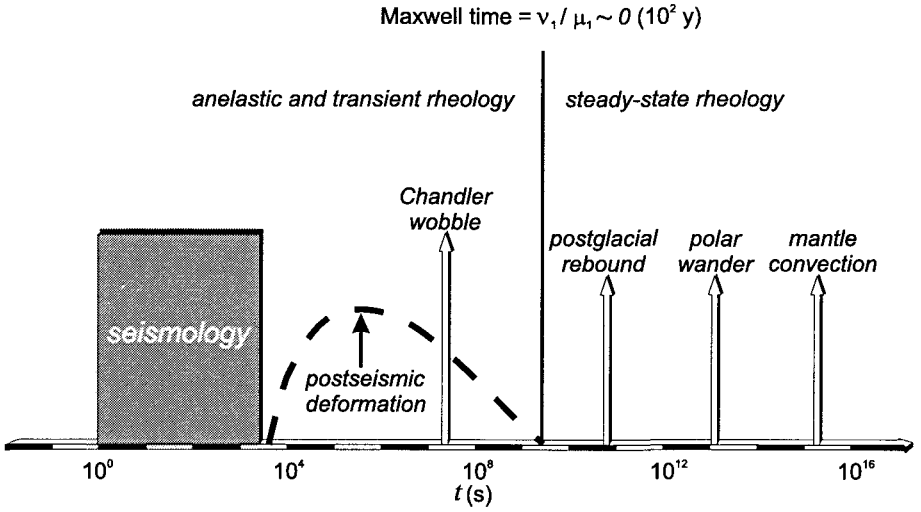

Figure 1.1. Diagram illustrating the relation of the characteristic time scale for several geophysical phenomena to the Maxwell time of the mantle defined as ν_1/μ_1 - with ν_1 and μ_1 denoting respectively the steady state mantle viscosity and rigidity - which separates the steady state and the transient regimes of mantle creep.

The appropriate constitutive relation which is to be employed in analyzing transient geodynamic phenomena, such as postglacial rebound or Glacial Isostatic Adjustment (GIA), is currently a matter of controversy in geophysics. Advocates of non-linear rheology (e.g., Melosh, 1980) use as supporting arguments the laboratory data of single-crystal olivine whose power law index is about three (Goetze, 1978; Durham and Goetze, 1977). But there is now mounting evidence that at the stress levels in postglacial rebound (less than $0(10^2$ bar)) the creep mechanism may in fact be linear for polycrystalline aggregates (Relandeau, 1981) since grain boundary processes, such as Coble creep , may become dominant. There are also recent theoretical studies indicating that the power law index changes gradually with stress and hence the transition stress which marks the boundary between linear and nonlinear behavior is not as sharply defined as has previously been thought (Greenwood *et al.*, 1980). Indeed, a proper mathematical formulation of the mixed initial and boundary-value problems associated with nonlinear viscoelasticity is a formidable one, fraught with numerical difficulties. It is also important to note that there is no unambiguous evidence in either the postglacial rebound event or in other types of geodynamic data which absolutely requires a nonlinear viscoelastic rheology, in spite of claims to the contrary. For these reasons, geophysicists tend to prefer the simple linear models in viscoelasticity, which allow for a considerably simpler mathematical treatment of the dynamics. Moreover, the

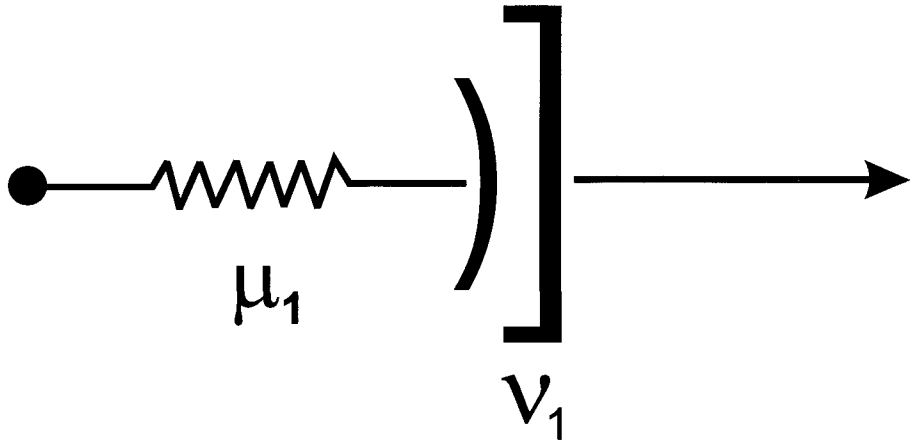

Figure 1.2. Mechanical analog of Maxwell rheology. The elastic response is governed by the shear modulus μ_1 of the spring while the long-term creep is controlled by the viscosity ν_1 of the dashpot.

linear approach also allows one to study easily the potentially interesting effects of the interaction between transient and steady-state rheologies. The simplest viscoelastic model which can describe the Earth as an elastic body for short time scales and as a viscous fluid for time scales characteristic of continental drift is that of a linear Maxwell solid. Figure 1.2 shows a standard one-dimensional spring and dashpot analog of the Maxwell rheology. The speed for shear wave propagation depends on the square root of the instantaneous rigidity μ_1, whereas the strength of mantle convection depends inversely upon the magnitude of the steady-state viscosity ν_1.

A powerful method of solving transient problems of linear viscoelasticity has been the use of the Correspondence Principle (Peltier, 1974), which allows one to employ the elastic solution of a given problem in the Laplace-transformed version of the corresponding viscoelastic problem. The Correspondence Principle for the Maxwell rheology and normal mode theory is introduced hereafter in this chapter.

2. MOMENTUM AND POISSON EQUATIONS

The following mathematical model describes the response of the viscoelastic linear Maxwell earth model to a delta function type of force. After having derived the Green functions , the response of the Earth to arbitrary loads or forces in space and time is found by convolving these functions with the loads or forces.

We assume that the rheological laws (stress - strain and stress - strain rate relations) are linear and that the strains are infinitesimal. We do not deal with non-linear rheologies and finite strain theory, but that does not imply that these are not important for the Earth Sciences. However, for a wide spectrum of solid-Earth relaxation processes, we can neglect both.

For long time scale processes the inertial forces vanish, and conservation of linear momentum requires that the body forces $\mathbf{F}$ per unit mass acting on the element of the body are balanced by the stresses that act on the surface of the element. At any instant of time we thus have for the stress tensor $\boldsymbol{\sigma}$ acting on the infinitesimal block with density ρ:

$$\nabla \cdot \boldsymbol{\sigma} + \rho \mathbf{F} = 0. \tag{1.1}$$

We assume first that the Earth is compressible , laterally homogeneous (but radially stratified!) and hydrostatically pre-stressed . We also assume that the Earth is not rotating (we will study rotation at a later stage). We will consider the elastic equations of motion , since any linear viscoelastic problem, which is of interest to us, is equivalent to an elastic problem in the Laplace domain , in agreement with the Correspondence Principle , as will be shown in the following. We thus solve the momentum and gravity equations for an elastic medium, and only at the last stage, once the elastic solution has been obtained, the Correspondence Principle is applied.

The stress tensor $\boldsymbol{\sigma}$ is the sum of the initial pressure, due to the hydrostatically prestressed conditions, plus a perturbation $\boldsymbol{\sigma}_1$, so that $\boldsymbol{\sigma}$ reads

$$\boldsymbol{\sigma} = \boldsymbol{\sigma}_1 - p_0 \mathbf{I}. \tag{1.2}$$

$\boldsymbol{\sigma}_1$ denotes a tensor which describes the acquired, non-hydrostatic stress, which will be related to the strain by means of the appropriate constitutive equations. The hydrostatic pressure p_0, with $\mathbf{I}$ the identity matrix, enters the equation above with the minus sign since it denotes a compressive stress, which is negative according to the convention that stresses are positive when they act in the same direction as the outward normal to the surface. On the elementary surface enclosing the elementary volume in which the equation of equilibrium holds, the stress due to the load of the overlying material, namely the pressure, is negative according to this convention. The equation of conservation of linear momentum thus reads

$$\nabla \cdot \boldsymbol{\sigma}_1 - \nabla p_0 + \rho \mathbf{F} = 0. \tag{1.3}$$

If the body is subject to an elastic displacement $\mathbf{u}$ in t_0, then the pressure in $t_0 + \delta t$ at a fixed point in space is given by

$$p_0(t_0 + \delta t) = p_0(t_0) - \mathbf{u} \cdot \nabla p_0. \tag{1.4}$$

The minus sign accounts for the fact that the pressure has to increase at a fixed point in space if the elastic displacement occurs in the opposite direction with respect to the pressure gradient.

The equation of conservation of linear momentum after the elastic displacement reads, with $p_0(t_0 + \delta t)$ instead of $p_0(t_0)$,

$$\nabla \cdot \boldsymbol{\sigma}_1 - \nabla p_0(t_0) + \nabla(\mathbf{u} \cdot \nabla p_0) + \rho \mathbf{F} = 0. \tag{1.5}$$

The gradient of the initial pressure is given by

$$\nabla p_0 = -\rho_0 g \hat{\mathbf{e}}_r, \tag{1.6}$$

where $\hat{\mathbf{e}}_r$ denotes the unit vector, positive outward from the Earth center. With this explicit expression of the gradient of the initial pressure, the equation of equilibrium becomes

$$\nabla \cdot \boldsymbol{\sigma}_1 - \nabla p_0(t_0) - \nabla(\rho_0 g \mathbf{u} \cdot \hat{\mathbf{e}}_r) + \rho \mathbf{F} = 0. \tag{1.7}$$

The force $\mathbf{F}$ can generally be split into gravity and all kinds of other forcings and loads (e.g., tidal forces, centrifugal forces, loads due to ice-water redistribution, earthquake forcings, etc.). Let us, for the moment, assume that the force $\mathbf{F}$ is gravity (so essentially the condition of a free, self-gravitating Earth with no other forcings or loads acting on its surface or interior) and that, as it is a conservative force, it can be expressed as the negative gradient of the potential field ϕ

$$\mathbf{F} = -\nabla \phi. \tag{1.8}$$

The potential field ϕ can be written as

$$\phi = \phi_0 + \phi_1, \tag{1.9}$$

with ϕ_0 as the field in the initial state and ϕ_1 the infinitesimal perturbation.

The linearized equation of momentum becomes, with ρ_1 the perturbation in the density and g the gravity,

$$\nabla \cdot \boldsymbol{\sigma}_1 - \nabla(\rho_0 g \mathbf{u} \cdot \hat{\mathbf{e}}_r) - \rho_0 \nabla \phi_1 - \rho_1 g \hat{\mathbf{e}}_r = 0, \tag{1.10}$$

since the second term of equation (1.7) is canceled by the term $-\rho_0 \nabla \phi_0$.

The first term of equation (1.10) describes the contribution from the stress, the second term the advection of the (hydrostatic) pre-stress, the third term the changed gravity (self-gravitation) and the fourth term the changed density (compressibility). In cases where self-gravitation is neglected, the third term will be zero, while in the case of incompressibility the fourth term will be zero.

The perturbed gravitational potential ϕ_1 satisfies the Poisson equation

$$\nabla^2\phi_1 = 4\pi G\rho_1, \tag{1.11}$$

with G as the universal gravitational constant . In the case of incompressibility the right-hand term will be zero since $\rho_1 = 0$, and equation (1.11) reduces to the Laplace equation

$$\nabla^2\phi_1 = 0. \tag{1.12}$$

The equations above need to be supplemented by a constitutive equation describing how stress and strain (or strain rate) are related to each other. Throughout this book we will make use of the Maxwell model depicted in Figure 1.2. The momentum and Poisson equations for an elastic solid will first be expanded in spherical harmonics and only afterwards the Correspondence Principle will be applied in order to retrieve the viscoelastic solution, which in our case is specialized for an incompressible material.

The equilibrium and Poisson equations can be written in spherical coordinates with r denoting the radial distance from the center of the Earth, θ the colatitude and ϕ the longitude (Schubert *et al.*, 2001, page 281), with derivatives with respect to r and θ denoted by ∂_r and ∂_θ. By assuming that there are no longitudinal components in the fields as well as in their derivatives, with symmetric deformation around the polar axis and taking account of the continuity equation written as follows

$$\rho_1 = -\nabla\cdot(\rho_0\mathbf{u}) = -\mathbf{u}\cdot\hat{\mathbf{e}}_r\,\partial_r\rho_0 - \rho_0\nabla\cdot\mathbf{u}, \tag{1.13}$$

with $\Delta = \nabla\cdot\mathbf{u}$ and ρ_1 denoting the perturbed density, the two r and θ components of the momentum and Poisson equations become

$$\begin{aligned}&-\rho_0\partial_r\phi_1 + \rho_0 g_0\Delta - \rho_0\partial_r(ug_0) + \partial_r\sigma_{rr}\\ &+r^{-1}\partial_\theta\sigma_{r\theta} + r^{-1}(2\sigma_{rr} - \sigma_{\theta\theta} - \sigma_{\phi\phi} + \sigma_{r\theta}\cot\theta) = 0\end{aligned} \tag{1.14}$$

$$\begin{aligned}&-\rho_0 r^{-1}\partial_\theta\phi_1 - \rho_0 g_0 r^{-1}\partial_\theta u\\ &+\partial_r\sigma_{r\theta} + r^{-1}\partial_\theta\sigma_{\theta\theta} + r^{-1}((\sigma_{\theta\theta} - \sigma_{\phi\phi})\cot\theta + 3\sigma_{r\theta}) = 0\end{aligned} \tag{1.15}$$

$$r^{-2}\partial_r(r^2\partial_r\phi_1) + (r^2\sin\theta)^{-1}\partial_\theta(\sin\theta\partial_\theta\phi_1) = -4\pi\,G(\rho_0\Delta + u\partial_r\rho_0), \tag{1.16}$$

where σ_{rr}, $\sigma_{\theta\theta}$, $\sigma_{\phi\phi}$ and $\sigma_{r\theta}$ denote the stress components in spherical coordinates expressed as

$$\sigma_{rr} = \lambda\Delta + 2\mu\epsilon_{rr} \tag{1.17}$$

$$\sigma_{\theta\theta} = \lambda\Delta + 2\mu\epsilon_{\theta\theta} \tag{1.18}$$

$$\sigma_{\phi\phi} = \lambda\Delta + 2\mu\epsilon_{\phi\phi} \tag{1.19}$$

$$\sigma_{r\theta} = 2\mu\epsilon_{r\theta}, \tag{1.20}$$

expressed in terms of the strain tensor components ϵ_{rr}, $\epsilon_{\theta\theta}$, $\epsilon_{\phi\phi}$, $\epsilon_{r\theta}$ and Lamé parameters λ and μ.

In this section we focus on the spheroidal components with the ϕ component of the displacement equal to zero. The strain tensor components are thus given in terms of the displacement

$$\epsilon_{rr} = \partial_r u \tag{1.21}$$

$$\epsilon_{\theta\theta} = r^{-1}(\partial_\theta v + u) \tag{1.22}$$

$$\epsilon_{\phi\phi} = r^{-1}(v\ \cot\theta + u) \tag{1.23}$$

$$\epsilon_{r\theta} = \frac{1}{2}(\partial_r v - r^{-1}v + r^{-1}\partial_\theta u), \tag{1.24}$$

where u and v denote the radial and tangential (along meridian) components of the displacement vector.

The r component of the momentum equations becomes in terms of the displacement components

$$\begin{aligned} &-\rho_0\partial_r\phi_1 + \rho_0 g\Delta - \rho_0\partial_r(ug) + \partial_r(\lambda\Delta + 2\mu\partial_r u) \\ &+\tfrac{\mu}{r^2}[4r\partial_r u - 4u + r(\partial_\theta\partial_r v + \partial_r v\cot\theta) \\ &+\partial_\theta^2 u + \partial_\theta u\cot\theta - 3(\partial_\theta v + v\cot\theta)] = 0. \end{aligned} \tag{1.25}$$

The θ component of the momentum equation is given by

$$\begin{aligned} &-(\tfrac{\rho_0}{r})\partial_\theta\phi_1 - (\tfrac{\rho_0 g}{r})\partial_\theta u + \mu\partial_r(\partial_r v - \tfrac{v}{r} + \tfrac{1}{r}\partial_\theta u) \\ &+\tfrac{1}{r}\partial_\theta(\lambda\Delta) + \tfrac{2\mu}{r^2}(\partial_\theta^2 v + \partial_\theta v\cot\theta - v\cot^2\theta - v) \\ &+\tfrac{3\mu}{r}\partial_r v + \tfrac{5\mu}{r^2}\partial_\theta u - \tfrac{\mu}{r^2}v = 0. \end{aligned} \tag{1.26}$$

The terms in equations (1.25) and (1.26) have been arranged in such a way as to make it easier the elimination of the derivatives with respect to the coordinate θ by making use of the Legendre equations and of its derivatives, once the fields u and v are expanded in Legendre polynomials, as done in section 1.3.

From equation (A.123) by Ben-Menahem and Singh (1981) we obtain the divergence of the displacement in spherical coordinates, which will be expanded in Legendre polynomials in the following section 1.3,

$$\nabla \cdot \mathbf{u} = \partial_r u + \frac{2}{r}u + \frac{1}{r}\partial_\theta v + \frac{cot\theta}{r}v. \tag{1.27}$$

3. EXPANSION IN SPHERICAL HARMONICS: SPHEROIDAL AND TOROIDAL SOLUTIONS

In principle, deformation, stress field and gravity field can be solved by means of numerical integration techniques from the three equations (1.16) and (1.25)-(1.26). However, we will see that it is also possible to solve these equations virtually analytically by means of normal model modeling in the Laplace-transformed domain, as stated by the Correspondence Principle. This kind of analytical solution has a few great advantages: it leads us to a deeper insight into the mechanisms of the relaxation process with additional checking possibilities, and certainly for spherical (global) models it often proves easier to be used than numerical integration techniques. Numerical integration techniques also have their advantages. For instance, they can generally deal more easily with more elaborate models (e.g., those that use non-linear rheologies or lateral variations) and often prove simpler to be used in half-space (regional) models, although also for half-space models analytical solutions are available (e.g., Wolf, 1985a,b). So the numerical and analytical models are to be seen as being more complementary than redundant.

Following our normal mode approach, the momentum equations (1.25)-(1.26) and the Poisson equation (1.16) must be expanded in spherical harmonics. Phinney and Burridge (1973) provide the methodology to expand any tensor field in spherical harmonics, defined by

$$Y_l^m(\theta,\phi) = (-1)^m P_l^m(cos\theta)\exp(im\phi), \tag{1.28}$$

with $l = 0, 1, 2, ...$ and $m = -l, -l+1, ...l$ and $P_l^m(cos\theta)$ denoting the associated Legendre function

$$P_l^m(cos\theta) = \frac{(1-cos^2\theta)^{m/2}}{2^l l!}\frac{d^{l+m}}{d(cos\theta)^{l+m}}(cos^2\theta - 1)^l. \tag{1.29}$$

Since our earth model is laterally homogeneous, the spheroidal solution does not contain any longitudinal component, and the spheroidal radial and tangential displacement components, the divergence Δ and the perturbation of the gravitational potential that will be used throughout are expanded in Legendre polynomials $P_l(cos\theta)$ rather than in spherical harmonics $Y_l^m(\theta,\phi)$. We thus

have for the spheroidal part the radial displacement u, the tangential (colatitudinal) component v, Δ and the perturbation in the gravitational potential ϕ_1 as functions of the scalars U_l, V_l, χ_l and ϕ_l, which depend solely on the harmonic degree l and on the radial distance r from the center of the Earth

$$u = \sum_{l=0}^{\infty} U_l(r) P_l^m(\cos\theta), \tag{1.30}$$

$$v = \sum_{l=0}^{\infty} V_l(r) \partial_\theta P_l(\cos\theta), \tag{1.31}$$

$$\Delta = \sum_{l=0}^{\infty} \chi_l(r) P_l(\cos\theta), \tag{1.32}$$

$$\phi_1 = -\sum_{l=0}^{\infty} \phi_l(r) P_l(\cos\theta), \tag{1.33}$$

where the Legendre polynomial $P_l(cos\theta)$ is obtained from the Rodrigues' formula

$$P_l(cos\theta) = \frac{1}{2^l l!} \frac{d^l}{d(cos\theta)^l} (cos^2\theta - 1)^l, \tag{1.34}$$

or from $m = 0$ in the previous definition (1.29) of the associated Legendre function. Note that the spheroidal solution does not carry any longitudinal displacement, as anticipated above.

The toroidal displacement components, v' along colatitude and w along longitude, are defined by the following expansion in spherical harmonics

$$v' = \sum_{l=0}^{\infty} W_l(r) \sum_{m=-l}^{l} \nabla_\phi Y_l^m(\theta, \phi) \tag{1.35}$$

$$w = -\sum_{l=0}^{\infty} W_l(r) \sum_{m=-l}^{m=l} \nabla_\theta Y_l^m(\theta, \phi), \tag{1.36}$$

which provide the toroidal components of the latitudinal and longitudinal displacements v' and w as a function of the W_l scalar harmonic coefficients. Collectively, U_l, V_l, W_l and ϕ_l are named scalar eigenfunctions and satisfy linear systems of homogeneous ordinary differential equations in the radial variable r.

3.1 SPHEROIDAL SOLUTION FOR THE INCOMPRESSIBLE CASE

By making use of the expansion of the spheroidal displacement components u, v, Δ and ϕ_1 defined in equations (1.30)-(1.33), of the Legendre equation

$$\frac{d^2}{d\theta^2}P_l(\theta) + \cot\theta\frac{d}{d\theta}P_l(\theta) = -l(l+1)P_l(\theta), \tag{1.37}$$

and of the derivative of the Legendre equation

$$\frac{d^3}{d\theta^3}P_l + \frac{d^2}{d\theta^2}P_l\cot\theta - \frac{d}{d\theta}P_l[1+\cot^2\theta] = -l(l+1)\frac{d}{d\theta}P_l, \tag{1.38}$$

the r and θ components of the momentum equations become for each harmonic degree l

$$\begin{aligned}&\rho_0\partial_r\phi_l + \rho_0 g\chi_l - \rho_0\partial_r(gU_l) + \partial_r(\lambda\chi_l + 2\mu\partial_r U_l)\\ &+r^{-2}\mu[4r\partial_r U_l - 4U_l + l(l+1)(-U_l - r\partial_r V_l + 3V_l)] = 0\end{aligned} \tag{1.39}$$

$$\begin{aligned}&\rho_0\phi_l - \rho_0 gU_l + \lambda\chi_l + r\mu\partial_r(\partial_r V_l - r^{-1}V_l + r^{-1}U_l)\\ &+r^{-1}\mu[5U_l + 3r\partial_r V_l - V_l - 2l(l+1)V_l] = 0.\end{aligned} \tag{1.40}$$

The Poisson equation becomes

$$\partial_r^2\phi_l + \frac{2}{r}\partial_r\phi_l - \frac{l(l+1)}{r^2}\phi_l = 4\pi G(\rho_0\chi_l + U_l\partial_r\rho_0). \tag{1.41}$$

The terms in the θ component of the momentum equation have been multiplied by r. The r and θ components of the momentum equations are expanded respectively on the Legendre polynomial P_l and on its derivative $\partial_\theta P_l$.

Once equations (1.39)-(1.41) are solved for each degree l, we obtain the fields summing up all the linearly independent solutions via equations (1.30)-(1.33).

For the divergence of the displacement Δ we obtain, by making use of equation (1.27) and of the Legendre equation,

$$\chi_l = \partial_r U_l + 2r^{-1}U_l - l(l+1)r^{-1}V_l. \tag{1.42}$$

The spheroidal solution vector $\mathbf{y}$ is defined as (Wu and Peltier, 1982)

$$
\begin{aligned}
y_1 &= U_l \\
y_2 &= V_l \\
y_3 &= \Pi_l + 2\mu\partial_r U_l \\
y_4 &= \mu(\partial_r V_l - \tfrac{V_l}{r} + \tfrac{U_l}{r}) \\
y_5 &= -\phi_l \\
y_6 &= -\partial_r \phi_l - \tfrac{(l+1)}{r}\phi_l + 4\pi G\rho_0 U_l,
\end{aligned}
\tag{1.43}
$$

where $\Pi_l = \lambda\chi_l$. The quantity y_6 is for obvious reasons sometimes nicknamed the potential stress. Why y_6 is chosen rather than $\partial_r\phi_l$ will become clear when the boundary conditions are discussed as follows.

From the condition of incompressibility

$$\chi_l = 0 \tag{1.44}$$

and homogeneity of each layer

$$\partial_r \rho_0 = 0, \tag{1.45}$$

we obtain the Laplace equation

$$\partial_r^2\phi_l + \frac{2}{r}\partial_r\phi_l - \frac{l(l+1)}{r^2}\phi_l = 0 \tag{1.46}$$

and momentum equations

$$
\begin{aligned}
&\rho_0\partial_r\phi_l - \rho_0\partial_r(gU_l) + \partial_r(\Pi_l + 2\mu\partial_r U_l) \\
&+\tfrac{\mu}{r^2}[4r\partial_r U_l - 4U_l + l(l+1)(-U_l - r\partial_r V_l + 3V_l)] = 0
\end{aligned}
\tag{1.47}
$$

$$
\begin{aligned}
&\rho_0\phi_l - \rho_0 g U_l + \Pi_l + \mu r\partial_r(\partial_r V_l - \tfrac{V_l}{r} + \tfrac{U_l}{r}) \\
&+\tfrac{\mu}{r}[5U_l + 3r\partial_r V_l - V_l - 2l(l+1)V_l] = 0,
\end{aligned}
\tag{1.48}
$$

where we have taken into account that the product $\lambda\chi_l$ remains finite for an incompressible body. From $\chi_l = 0$ we obtain the following relationship between the tangential and radial components of the displacement

$$V_l = \frac{r\partial_r U_l + 2U_l}{l(l+1)} \tag{1.49}$$

once we make use of the condition of incompressibility $\nabla \cdot \mathbf{u} = 0$.

Exercise. Prove that, with the above definition of solution vector (1.43), the momentum and Laplace equations for the incompressible case can be cast in the matrix form

$$\frac{d}{dr}\mathbf{y} = \mathbf{A}\cdot\mathbf{y}, \tag{1.50}$$

where the matrix $\mathbf{A}_l(r)$ reads

$$\begin{pmatrix}
-\frac{2}{r} & \frac{l(l+1)}{r} & 0 & 0 & 0 & 0 \\
-\frac{1}{r} & \frac{1}{r} & 0 & \frac{1}{\mu} & 0 & 0 \\
\frac{4}{r}\left(\frac{3\mu}{r}-\rho_0 g\right) & -\frac{l(l+1)}{r}\left(\frac{6\mu}{r}-\rho_0 g\right) & 0 & \frac{l(l+1)}{r} & -\frac{\rho_0(l+1)}{r} & \rho_0 \\
-\frac{1}{r}\left(\frac{6\mu}{r}-\rho_0 g\right) & \frac{2(2l^2+2l-1)\mu}{r^2} & -\frac{1}{r} & -\frac{3}{r} & \frac{\rho_0}{r} & 0 \\
-4\pi G\rho_0 & 0 & 0 & 0 & -\frac{l+1}{r} & 1 \\
-\frac{4\pi G\rho_0(l+1)}{r} & \frac{4\pi G\rho_0 l(l+1)}{r} & 0 & 0 & 0 & \frac{l-1}{r}
\end{pmatrix}, \tag{1.51}$$

with the gravity $g = 4\pi G\rho_0 r/3$.

Deriving equation (1.47) with respect to r and summing the result of this derivation to (1.47) multiplied by $2/r$ and to (1.48) multiplied by $-l(l+1)/r^2$, we obtain

$$\begin{aligned}
&\nabla_r^2(\rho_0\phi_l - \rho_0 g U_l + \Pi_l) = -2\mu\partial_r^3 U_l - \tfrac{8}{r^2}\mu\partial_r^2 U_l \\
&+\tfrac{2l(l+1)}{r^2}\mu\partial_r U_l + \tfrac{4l(l+1)}{r^3}\mu U_l + \tfrac{2l(l+1)}{r^2}\mu\partial_r^2 V_l - \tfrac{2[l(l+1)]^2}{r^3}\mu V_l
\end{aligned} \tag{1.52}$$

and finally, making use of equation (1.49) derived twice with respect to r in order to eliminate $\partial_r^3 U_l$, we obtain

$$\nabla_r^2(\rho_0\phi_l - \rho_0 g U_l + \Pi_l) = 0, \tag{1.53}$$

where

$$\nabla_r^2 = \partial_r^2 + \frac{2}{r}\partial_r - \frac{l(l+1)}{r^2}, \tag{1.54}$$

which is equation (25) in Wu and Peltier (1982), multiplied by ρ_0.

From (1.47) by collecting the derivative with respect to r,

$$\begin{aligned}
&\partial_r(\rho_0\phi_l - \rho_0 g_0 U_l + \Pi_l) = -2\mu\partial_r^2 U_l \\
&-\tfrac{\mu}{r^2}[4r\partial_r U_l - 4U_l + l(l+1)(-U_l - r\partial_r V_l + 3V_l)],
\end{aligned} \tag{1.55}$$

which can be rearranged as follows

$$\begin{aligned}&\partial_r(\rho_0\phi_l - \rho_0 g_0 U_l + \Pi_l) = -2\mu\partial_r^2 U_l \\ &-\tfrac{\mu}{r^2}[4r\partial_r U_l - 4U_l - l(l+1)U_l - rl(l+1)\partial_r V_l + 3l(l+1)V_l],\end{aligned} \tag{1.56}$$

which becomes with equation (1.49)

$$\partial_r(\rho_0\phi_l - \rho_0 g_0 U_l + \Pi_l) = -\mu\partial_r^2 U_l - 4\frac{\mu}{r}\partial_r U_l - 2\frac{\mu}{r^2}U_l + \frac{\mu}{r^2}l(l+1)U_l. \tag{1.57}$$

Multiplying equation (1.55) by r^2 and taking into account equation (1.57) yields, after having changed sign in each term,

$$r^2\partial_r(\rho_0 g U_l - \Pi_l - \rho_0\phi_l) = \mu r^2\partial_r^2 U_l + 4\mu r\partial_r U_l + 2\mu U_l - \mu l(l+1)U_l. \tag{1.58}$$

We define

$$\rho_0 g U_l - \rho_0\phi_l - \Pi_l = \Gamma_l. \tag{1.59}$$

Exercise. Show that the solution of the Laplace equation (1.46) takes the form

$$\phi = c_3 r^l + c_3^* r^{-(l+1)}, \tag{1.60}$$

where r^l denotes the regular solution in $r = 0$ and $r^{-(l+1)}$ denotes the singular one. The subscript 3 in equation (1.60) is used for convenience.

Γ_l satisfies the Laplace equation (1.53) and thus takes the following form, with the same dependence of ϕ_l with respect to r, where the constants c_1 and c_1^*, with subscript 1, are multiplied by μ for convenience, as will be apparent in the following

$$\Gamma_l = \mu c_1 r^l + \mu c_1^* r^{-(l+1)}. \tag{1.61}$$

The homogeneous equation

$$r^2\partial_r^2 U_l + 4r\partial_r U_l + 2U_l - l(l+1)U_l = 0, \tag{1.62}$$

obtained from equation (1.57) with the left member set to zero, has two solutions, a regular one

$$U_l' = c_2 r^{(l-1)} \tag{1.63}$$

and a singular one

$$U_l'' = c_2^* r^{-(l+2)}. \tag{1.64}$$

A particular solution for the regular component can be obtained by substituting the regular component of Γ, providing

$$r^2\partial_r^2 U_l + 4r\partial_r U_l + 2U_l - l(l+1)U_l = r^2 c_1 l r^{(l-1)}. \tag{1.65}$$

The regular solution is thus

$$U_l''' = \frac{c_1 l}{2(2l+3)} r^{(l+1)}. \tag{1.66}$$

The singular component of the solution becomes, with the same procedures, becomes

$$U_l'''' = c_1^* \frac{(l+1)}{2(2l-1)} r^{-l}. \tag{1.67}$$

Summing up all the contributions, we obtain

$$U_l = c_1 \frac{l r^{(l+1)}}{2(2l+3)} + c_2 r^{(l-1)} + c_1^* \frac{(l+1)}{2(2l-1)} r^{-l} + c_2^* r^{-(l+2)}. \tag{1.68}$$

From equation (1.68) and (1.49) we obtain the horizontal component of the displacement

$$V_l = c_1 \tfrac{l+3}{2(2l+3)(l+1)} r^{l+1} + c_2 \tfrac{r^{l-1}}{l} + c_1^* \tfrac{2-l}{2l(2l-1)} r^{-l} - c_2^* \tfrac{r^{-(l+2)}}{l+1}. \tag{1.69}$$

Exercise. Verify that with the definitions of the solution vector (1.43) the components y_3, y_4 and y_6 take the form

$$\begin{aligned} y_3 = {} & c_1 \left[\tfrac{(l\rho_0 gr + 2(l^2-l-3)\mu) r^l}{2(2l+3)}\right] + c_2[\rho_0 gr + 2(l-1)\mu) r^{l-2}]] \\ & + c_3 \left[-\rho_0 r^l\right] + c_1^* \left[\tfrac{(l+1)\rho_0 gr - 2(l^2+3l-1)\mu}{2(2l-1) r^{l+1}}\right] \\ & + c_2^* \left[\tfrac{\rho_0 gr - 2(l+2)\mu}{r^{l+3}}\right] + c_3^* \left[-\rho_0 r^{-(l+1)}\right] \end{aligned} \tag{1.70}$$

$$\begin{aligned} y_4 = {} & c_1 \tfrac{l(l+2)}{(2l+3)(l+1)} r^l + c_2 \tfrac{2(l-1)}{l} r^{(l-2)} \\ & + c_1^* \tfrac{(l^2-1)}{l(2l-1)} r^{-(l+1)} + c_2^* \tfrac{2(l+2)}{l+1} r^{-(l+3)} \end{aligned} \tag{1.71}$$

$$y_6 = +c_1 \frac{2\pi G\rho l r^{l+1}}{(2l+3)} + c_2 4\pi G\rho_0 r^{l-1} - c_3(2l+1)r^{l-1}$$
$$+c_1^* \frac{2\pi G(l+1)}{(2l-1)} r^{-l} + 4\pi G\rho_0 c_2^* r^{-(l+2)}. \tag{1.72}$$

For each of the N layers of the earth model (assuming that each layer has material parameters which are constant inside it and that gravity g is constant inside such a layer), on the basis of equations (1.60), (1.68) - (1.72) the solution can thus be written as

$$\mathbf{y}(r) = \mathbf{Y}_l(r) \cdot \mathbf{C}_l, \tag{1.73}$$

in which $\mathbf{Y}_l$ is the fundamental matrix and $\mathbf{C}_l$ a 6-component vector integration constant.

The fundamental matrix $\mathbf{Y}_l(r,s)$ reads

$$\begin{pmatrix}
\frac{lr^{l+1}}{2(2l+3)} & r^{l-1} & 0 & \\
\frac{(l+3)r^{l+1}}{2(2l+3)(l+1)} & \frac{r^{l-1}}{l} & 0 & \\
\frac{(l\rho_0 gr+2(l^2-l-3)\mu)r^l}{2(2l+3)} & (\rho_0 gr+2(l-1)\mu)r^{l-2} & -\rho_0 r^l & \\
\frac{l(l+2)\mu r^l}{(2l+3)(l+1)} & \frac{2(l-1)\mu r^{l-2}}{l} & 0 & \cdots \\
0 & 0 & -r^l & \\
\frac{2\pi G\rho_0 l r^{l+1}}{2l+3} & 4\pi G\rho_0 r^{l-1} & -(2l+1)r^{l-1} &
\end{pmatrix}$$

$$\begin{pmatrix}
\frac{(l+1)r^{-l}}{2(2l-1)} & r^{-l-2} & 0 \\
\frac{(2-l)r^{-l}}{2l(2l-1)} & -\frac{r^{-l-2}}{l+1} & 0 \\
\frac{(l+1)\rho_0 gr-2(l^2+3l-1)\mu}{2(2l-1)r^{l+1}} & \frac{\rho_0 gr-2(l+2)\mu}{r^{l+3}} & -\frac{\rho_0}{r^{l+1}} \\
\frac{(l^2-1)\mu}{l(2l-1)r^{l+1}} & \frac{2(l+2)\mu}{(l+1)r^{l+3}} & 0 \\
0 & 0 & -\frac{1}{r^{l+1}} \\
\frac{2\pi G\rho_0(l+1)}{(2l-1)r^l} & \frac{4\pi G\rho_0}{r^{l+2}} & 0
\end{pmatrix} \tag{1.74}$$

Each column of this fundamental matrix represents an independent solution of the system (1.50) of ordinary differential equations. The analytical expression of the fundamental solution, which includes the regular and singular part in $r = 0$, was first obtained in Sabadini *et al.* (1982a), while the regular part, which is appropriate for the solution of a homogeneous, viscoelastic sphere, was first obtained by Wu and Peltier (1982). The inverse of the fundamental matrix $\mathbf{Y}_l$ has the form

$$\mathbf{Y}_l^{-1}(r) = \mathbf{D}_l(r)\bar{\mathbf{Y}}_l(r), \tag{1.75}$$

with $\mathbf{D}$ being a diagonal matrix with elements

$$\begin{aligned} &\mathrm{diag}(\mathbf{D}_l(r)) = \\ &\tfrac{1}{2l+1}\left(\tfrac{l+1}{r^{l+1}}\,,\ \tfrac{l(l+1)}{2(2l-1)r^{l-1}}\,,\ -\tfrac{1}{r^{l-1}}\,,\ lr^l\,,\ \tfrac{l(l+1)}{2(2l+3)}r^{l+2}\,,\ -r^{l+1}\right) \end{aligned} \tag{1.76}$$

and

$$\bar{\mathbf{Y}}_l(r) = \begin{pmatrix} \frac{\rho g r}{\mu} - 2(l+2) & 2l(l+2) & -\frac{r}{\mu} & \frac{lr}{\mu} & \frac{\rho r}{\mu} & 0 \\ -\frac{\rho g r}{\mu} + \frac{2(l^2+3l-1)}{l+1} & -2(l^2-1) & \frac{r}{\mu} & \frac{(2-l)r}{\mu} & -\frac{\rho r}{\mu} & 0 \\ 4\pi G\rho & 0 & 0 & 0 & 0 & -1 \\ \frac{\rho g r}{\mu} + 2(l-1) & 2(l^2-1) & -\frac{r}{\mu} & -\frac{(l+1)r}{\mu} & \frac{\rho r}{\mu} & 0 \\ -\frac{\rho g r}{\mu} - \frac{2(l^2-l-3)}{l} & -2l(l+2) & \frac{r}{\mu} & \frac{(l+3)r}{\mu} & -\frac{\rho r}{\mu} & 0 \\ 4\pi G\rho r & 0 & 0 & 0 & 2l+1 & -r \end{pmatrix} \tag{1.77}$$

Although it would be quite laborious to derive such an analytical compact form of a 6×6 inverse matrix 'by hand', this can be done nowadays by means of an algebraic software package like *Mathematica*. It was first done by Spada *et al.* (1990, 1992b). Of course, it is not difficult to show analytically that $\mathbf{Y}_l \times \mathbf{Y}_l{}^{-1} = \mathbf{I}$, with $\mathbf{I}$ the identity matrix, by hand! Appendix A provides the elements of the fundamental matrix for the compressible case (Vermeersen *et al.*, 1996b).

3.2 TOROIDAL SOLUTION FOR THE INCOMPRESSIBLE CASE

With the following definition of the toroidal vector solution $\mathbf{y}$

$$y_1 = W_l \tag{1.78}$$

$$y_2 = \mu\left(\frac{dW_l}{dr} - \frac{W_l}{r}\right), \tag{1.79}$$

the toroidal differential equations take the following form for each harmonic degree l

$$\frac{d}{dr}\mathbf{y} = \mathbf{A} \cdot \mathbf{y}. \tag{1.80}$$

where the $\mathbf{A}$ matrix has been obtained by Alterman *et al.* (1959)

$$\mathbf{A}_l(r) = \begin{pmatrix} \frac{1}{r} & \frac{1}{\mu} \\ \frac{\mu(l(l+1)-2)}{r^2} & \frac{-3}{r} \end{pmatrix}. \tag{1.81}$$

Exercise. Show that the l component of the fundamental solution for the toroidal solution is given by

$$\mathbf{Y}_l(r) = \begin{pmatrix} r^l & r^{-l-1} \\ \mu(l-1)r^{l-1} & -\mu(s)(l+2)r^{-l-2} \end{pmatrix}. \tag{1.82}$$

The inverse matrix of the fundamental toroidal solution reads

$$\mathbf{Y}_l^{-1}(r) = \begin{pmatrix} \frac{2+l}{r^l(1+2l)} & \frac{r^{1-l}}{\mu(1+2l)} \\ \frac{r^{1+l}(l-1)}{1+2l} & \frac{r^{2+l}}{-\mu(1+2l)} \end{pmatrix}. \tag{1.83}$$

4. FUNDAMENTAL SPHEROIDAL MATRIX IN THE LAPLACE DOMAIN

The Laplace transform $\tilde{f}(s)$ of a function $f(t)$ is defined by

$$\tilde{f}(s) = \int_0^\infty f(t)e^{-st}dt, \tag{1.84}$$

with t as time and s the Laplace variable (which has the dimension of inverse time). It is straightforward to show that the Laplace transform of the time derivative df/dt of the function $f(t)$ is $s\tilde{f}(s)$.

All the results shown in this book are based on the incompressible viscoelastic Maxwell solid, which means that only the rigidity μ enters the fundamental solution (see equation (1.74)). We can thus make use of the one-dimensional relationship between the stress and strain rate for a Maxwell solid depicted in Figure 1.2 as given by

$$\frac{d\epsilon}{dt} = \frac{\sigma}{2\nu} + \frac{1}{2\mu}\frac{d\sigma}{dt}, \tag{1.85}$$

with ν being the viscosity of the dashpot (of the mantle, for the case of the Earth!). Laplace transformation of the equation above leads to

$$\tilde{\sigma}_{ij}(s) = 2\tilde{\mu}(s)\tilde{\epsilon}_{ij}(s), \tag{1.86}$$

with the Laplace-transformed Lamé parameter $\mu(s)$ being

$$\tilde{\mu}(s) = \frac{\mu s}{s + \mu/\nu}. \tag{1.87}$$

Note that equation (1.86) has the form of a Hookean (linearly elastic) equation in the Laplace-transformed domain. This is a very important aspect and greatly facilitates calculations. So we can derive equations for linear Maxwell viscoelastic bodies in the time domain with formulas for linear Hooke elastic bodies in the Laplace-transformed domain. It can be shown that this is generally valid for all linear viscoelastic bodies (so also, e.g., the Kelvin-Voigt and Burgers models in Ranalli, 1995). The so-called Correspondence Principle states that by calculating the associated elastic solutions in the Laplace-transformed domain the time dependent viscoelastic solutions can be found by Laplace inversion in a unique way. From now on, in the other sections of this chapter, the tilde over the quantities will be neglected in order not to overwhelm the text, although all the equations and quantities are defined in the Laplace-transformed domain.

5. PROPAGATOR MATRIX TECHNIQUE

For each layer of a spherical earth model, the solution vector (1.43) can be determined from the fundamental matrix. This solution vector expresses the most general solution for displacements (radial and horizontal), stresses (radial and tangential), gravity and y_6, from which the gravity gradient can be derived for each layer of the spherical model and for each harmonic degree l in the Laplace domain. Each viscoelastic layer of the model is bounded by either another internal viscoelastic layer or an external layer (free outer surface, inviscid outer core layer at the core-mantle boundary (CMB)). For each of these cases we need to determine the boundary conditions.

The internal boundary conditions are quite easy: for a boundary between two elastic or viscoelastic layers we require that U_l, V_l, σ_{rrl}, $\sigma_{r\theta l}$ and ϕ_l be continuous. This implies that during deformation there will be no 'cavitation' and no slip, while it is also assumed that no material crosses the boundary. Internal boundaries where no material crosses are called chemical boundaries. Internal boundaries where material does cross, undergoing a phase change, are called phase-change boundaries. The boundary between the upper mantle and lower mantle at about 670 km depth is likely to be partly a chemical and partly a phase-change boundary, but we will assume first that in our earth models there are only chemical boundaries. In the following section 1.7, phase-change boundaries will also be tackled.

As was already alluded to when y_6 was defined in equation (1.43), we do not take the gravity gradient as sixth component of the vector but a combination of gravity, gravity gradient and radial displacement. The reason becomes clear when the boundary condition for the gravity gradient at the free outer surface of the model is considered. If ϕ^e denotes the external potential and ϕ the potential evaluated in the top layer of the earth model, then applying the Gauss theorem at the Poisson equation within a volume embedded in a pill-box at the free

surface, with $\rho_1 = -\rho_0 \nabla \cdot \mathbf{u}$ from equation (1.13), the surface layer being homogeneous in density, we obtain

$$\frac{\partial \phi_l^e}{\partial r} - \frac{\partial \phi_l}{\partial r} = -4\pi G \rho U_l. \tag{1.88}$$

Only the radial component of the gravitational potential and the radial component of the displacement contribute to the surface integral.

The gravity gradient of the external layer resulting from the term in $r^{-(l+1)}$ from equation (1.60) satisfies

$$\frac{\partial \phi_l^e}{\partial r} = -\frac{l+1}{r}\phi_l^e. \tag{1.89}$$

The contribution from the other term from equation (1.60), proportional to r^l, becomes irregular at infinity and must be excluded. We also have

$$\phi_l^e = \phi_l, \tag{1.90}$$

so that we can express the external boundary condition as

$$y_6 = -\frac{\partial \phi}{\partial r} - \frac{l+1}{r}\phi + 4\pi G \rho U_l = 0. \tag{1.91}$$

With this it is clear that also y_6 is continuous for internal boundaries between viscoelastic layers.

5.1 PROPAGATION OF THE SPHEROIDAL SOLUTION

Due to the continuity of the fields y_j $(j = 1, 2, 3, 4, 5, 6)$ at the interface $r = r_{i+1}$, the top layer i, in which

$$\mathbf{y}^{(i)}(r_{i+1}, s) = \mathbf{Y}^{(i)}(r_{i+1}, s)\mathbf{C}^{(i)}, \tag{1.92}$$

can be linked to the layer $i + 1$ below it, with

$$\mathbf{y}^{(i+1)}(r_{i+1}, s) = \mathbf{Y}^{(i+1)}(r_{i+1}, s)\mathbf{C}^{(i+1)} \tag{1.93}$$

by assuming the continuity of the components of the solution vector

$$\mathbf{y}^{(i)} = \mathbf{y}^{(i+1)} \tag{1.94}$$

as a consequence of the boundary conditions at the internal boundaries. The subscript l denoting the harmonic degree is deleted from now on, in order to not overwhelm the notation. With equations (1.92)-(1.94) it is possible to express the unknown constant vector $\mathbf{C}^{(i)}$ in terms of the unknown constant vector $\mathbf{C}^{(i+1)}$. By doing this for every internal boundary of an N layer model (layer 1

is the top layer [crust or lithosphere], layers $2, 3, ..., N-1$ the layers below it, and layer N the core), the solution vector at the surface of the Earth at $r_1 = a$ can be related to the conditions $\mathbf{C}_l^{(N)}(r_c)$ at the core-mantle boundary (CMB) $r_N = r_c$ as

$$\mathbf{y}(a,s) = \left(\prod_{i=1}^{N-1} \mathbf{Y}^{(i)}(r_i,s)\mathbf{Y}^{(i)^{-1}}(r_{i+1},s) \right) \mathbf{Y}^{(N)}(r_c,s)\mathbf{C}^{(N)}. \quad (1.95)$$

The conditions at the CMB have been disputed among geophysicists since the 1960's. This controversy focuses on the treatment of the continuity conditions for the vertical deformation at the CMB. Without going into details, if it is required that the vertical deformation at the CMB be continuous, then this restricts the core to being either in a state of neutral equilibrium (homogeneous with neutral adiabatic temperature gradient) or that the radial stress at the CMB is zero. Both could be the case, but such restrictions are obviously not always the case in reality. Therefore the vertical deformation should in general not be continuous at the CMB. This might seem strange, as one would think that this could lead to 'cavitation' or to the overlapping of layers. The way out of this conundrum is that the fluid core layers are rather to be interpreted as equipotentials rather than material layers.

Gravity should be continuous at the CMB, at least if we assume that there are no additional masses positioned at the CMB. Inside the core, gravity should be proportional to r^l, as the other solution of equation (1.60) is irregular at the center of the Earth. So for the lowermost mantle layer at the CMB we get

$$y_5^{(N)}(r_c) = K_1 r_c^l, \quad (1.96)$$

with K_1 a constant.

Assuming that the core is inviscid (fluid) , we can readily deduce that the tangential displacement of the mantle is not restricted, so for the lowermost mantle layer at the CMB we have

$$y_2^{(N)}(r_c) = K_2, \quad (1.97)$$

with K_2 as a constant and $y_2^{(N)}$ the second component of the vector $\mathbf{y}^{(N)}$.

The following condition holds for the lowermost mantle layer at the CMB, where the first term provides the radial displacement of the equipotential ϕ/g_c (note the minus sign of ϕ in (1.43))

$$y_1^{(N)}(r_c) = -\frac{y_5^{(N)}}{g_c} + K_3 = -\frac{3r_c^{l-1}}{4\pi G\rho_c} K_1 + K_3, \quad (1.98)$$

with g_c being the gravity at the CMB, K_3 a constant, ρ_c the density of the core and $y_1^{(N)}$ the first component of the vector $\mathbf{y}^{(N)}$.

The radial stress (pressure) should be continuous over the CMB. This leads for the lowermost mantle layer at the CMB to the condition

$$y_3^{(N)}(r_c) = g_c \rho_c K_3 = \frac{4}{3}\pi G \rho_c^2 r_c K_3, \tag{1.99}$$

with $y_3^{(N)}$ the third component of the vector $\mathbf{y}^{(N)}$.

The tangential stress in the fluid core is zero, and thus continuity of stress requires for the lowermost mantle layer at the CMB that

$$y_4^{(N)}(r_c) = 0, \tag{1.100}$$

with $y_4^{(N)}$ as the fourth component of the vector $y^{(N)}$.

Finally, y_6 should also be continuous at the CMB, leading for the lowermost mantle layer at the CMB to the condition

$$y_6^{(N)}(r_c) = 2(l-1) r_c^{l-1} K_1 + 4\pi G \rho_c K_3, \tag{1.101}$$

with $y_6^{(N)}$ as the sixth component of the vector $\mathbf{y}^{(N)}$.

If we treat the core as the innermost layer, then the conditions at the CMB can be expressed as a 6×3 interface matrix $\mathbf{I}_c(r_c)$ as

$$\mathbf{Y}^{(N-1)}(r_c, s)\mathbf{C}^{(N-1)}(r_c) = \mathbf{I}_c(r_c)\mathbf{C}_c, \tag{1.102}$$

with

$$\mathbf{I}_c(r_c) = \begin{pmatrix} -r_c^{l-1}/A_c & 0 & 1 \\ 0 & 1 & 0 \\ 0 & 0 & \rho_c A_c r_c \\ 0 & 0 & 0 \\ r_c^l & 0 & 0 \\ 2(l-1) r_c^{l-1} & 0 & 3A_c \end{pmatrix}, \tag{1.103}$$

with ρ_c being the (uniform) density of the core, $A_c = \frac{4}{3}\pi G \rho_c$, and $\mathbf{C}_c = (K_1, K_2, K_3)$ a 3-component constant vector.

The solution vector $\mathbf{y}(a, s)$, equation (1.95), with (1.103) can be used to express either the conditions for a free surface, or the conditions for a surface or internal loading. The loading/forcing case will be treated afterwards.

The solution vector $\mathbf{y}(a, s)$ can be split into two parts: one that contains the unconstrained parameters U_l, V_l and ϕ_l (which we are solving for), and the other containing the constrained $y_3 = \sigma_{rr}$, $y_4 = \sigma_{r\theta}$ and y_6.

For a free surface, the components of the latter, as we have already seen, are all zero at the surface. If $\mathbf{P}_1$ denotes the projection operator on the third, fourth and sixth components of the solution vector given by equation (1.43), then we get the following condition

$$0 = \mathbf{P}_1 \mathbf{y}(a,s) = \mathbf{P}_1 \left(\prod_{i=1}^{N-1} \mathbf{Y}^{(i)}(r_i,s) \mathbf{Y}^{(i)^{-1}}(r_{i+1},s) \right) \mathbf{I}_c(r_c) \mathbf{C}_c, \quad (1.104)$$

with $\mathbf{P}_1$ the projection operator

$$\mathbf{P}_1 = \begin{pmatrix} 0 & 0 & 0 & 0 & 0 & 0 \\ 0 & 0 & 0 & 0 & 0 & 0 \\ 0 & 0 & 1 & 0 & 0 & 0 \\ 0 & 0 & 0 & 1 & 0 & 0 \\ 0 & 0 & 0 & 0 & 0 & 0 \\ 0 & 0 & 0 & 0 & 0 & 1 \end{pmatrix}. \quad (1.105)$$

This condition constrains the s-values in the sense that only those s-values for which

$$\det \left(\mathbf{P}_1 \left(\prod_{i=1}^{N-1} \mathbf{Y}^{(i)}(r_i,s) \mathbf{Y}^{(i)^{-1}}(r_{i+1},s) \right) \mathbf{I}_c(r_c) \right) = 0 \quad (1.106)$$

are non-zero solutions of equation (1.104). The expression given by equation (1.106) is called the secular equation and the determinant the secular determinant. Its solutions $s = s_j$ $(j = 1,2,3,...,M)$ are the inverse relaxation times of the M relaxation modes of the earth model. These s_j are dependent on the harmonic degree l (and thus must be determined for each harmonic degree), but the index l has been left out in order not to complicate the indexing. The total number of relaxation modes M for each harmonic degree is the same for each harmonic degree (with the exception of degree 1, but we will not digress any further on the differences between degree 1 on the one hand and degrees 2 and higher on the other).

Experience and (extremely laborious) analytical proofs have led to the following results:

- The surface contributes one mode, labeled $M0$.
- If there is an elastic lithosphere on top of a viscoelastic mantle, then there is one mode triggered by the lithosphere-mantle boundary, labeled $L0$.
- At the boundary of two viscoelastic layers, one buoyancy mode is triggered if the density on both sides of the boundary is different. Buoyancy modes between two mantle layers are usually labeled Mi, with $i = 1,2,3,...,$ whereby $M1$ is usually the buoyancy mode associated with the 670 km discontinuity (upper / lower mantle) and $M2$ with the 400 km discontinuity (shallow upper mantle / mantle transition zone).

- At the same boundary two additional viscoelastic modes are triggered if the Maxwell time on both sides of the boundary is different (so if the viscosity and rigidity are different, but the ratio of viscosity and rigidity is not, then these viscoelastic modes are absent). These 'paired' modes are also called transient modes as they have relatively short relaxation times and are therefore usually labeled T_i, with $i = 1, 2, 3, ...$
- The boundary between the lowermost mantle layer and the inviscid core contributes one mode, labeled $C0$.

It is thus possible, with the above rules, to determine the total number of modes of equation (1.106). This is of importance as solving this equation has to be done numerically. However, this root-solving is the only non-analytical part of the viscoelastic relaxation method as described in this chapter.

The root-solving procedure usually consists of two parts: grid-spacing, followed by a bisection algorithm. In the grid-spacing part, the s-domain is split into a number of discrete intervals. For each s-value at a boundary of an interval, the value of the determinant expressed by equation (1.106) is calculated, after which this value is multiplied with the value of the determinant of the s-value of the boundary next to it. If this product is positive, then the determinant has not changed in sign (or has changed an even number of times). If the product is negative, then we are sure that there is (at least) one root inside the interval bounded by the two s-values for which the determinant was calculated. In that case, the interval is split up in two parts, and the procedure of determining the product of the determinant of the bounding s-values is repeated. The interval where the determinant changes sign will result again in a negative product, and for this interval the procedure of cutting the interval in two, etc., is repeated. Thus the s-value where the determinant (1.106) is equal to zero becomes progressively better estimated with each further step in this bisection algorithm. Of course, it can happen that the determinant (1.106) changes sign over a small s-interval twice or even more times. It is thus necessary to choose small grids in the s-domain (in practice, it appears that especially the two modes of each T-mode pair have inverse relaxation times (s-values) that are very close to each other). Only after the complete number (determined with the rules above) of roots/modes of equation (1.106) has been found can one be sure that the complete signal will be retrieved after inverse-Laplace transformation. For this final step in the relaxation modeling procedure we use the so-called method of complex contour integration. Those readers who are not acquainted with this technique will find an overview in Appendix B.

5.2 PROPAGATION OF THE TOROIDAL SOLUTION

The same procedure discussed above can be used to propagate the toroidal solution. At the CMB the boundary condition is

$$y_2(c) = 0, \tag{1.107}$$

which states that at the core-mantle boundary the tangential stresses are zero (Smylie and Manshina, 1971).

Exercise. On analogy with the spheroidal case, it is possible to build $\mathbf{I}_c(r_c)$, which is now a vector, so as to make use of the same propagation procedure described for the spheroidal case. Making use of the boundary condition at the CMB for the tangential stress shows that $\mathbf{I}_c(r_c)$ takes the form

$$\mathbf{I}_c(r_c) = \begin{pmatrix} \frac{(l-1)r_c^{3l+1}}{l+2} + r_c^{-(l+1)} \\ 0 \end{pmatrix}. \tag{1.108}$$

6. INVERSE RELAXATION TIMES FOR INCOMPRESSIBLE EARTH MODELS

In order to gain insights into the physics of the relaxation processes, it is important to take a close look at the relaxation times corresponding to the modes excited by discontinuities in the physical parameters of simple earth models. We will consider the spheroidal case. The relaxation times for the five layer model, depicted in Figure 1.3, panel (a), are shown in Figures 1.4 and 1.5 as a function of the harmonic degree l. A simpler 4-layer model is shown in Figure 1.3, panel (b), for comparison.

The relaxation times $T_r = -1/s_i$ are expressed in years, ranging from $l = 2$ to $l = 100$. Figure 1.4 deals with a viscosity increase in the lower mantle, with the ratio B between the lower and upper mantle viscosity ranging from 1 to 200. OM stands for an old viscosity model in which the upper mantle viscosity is fixed at 10^{21} Pa s, while NM stands for a new viscosity model in which ν_1 is fixed at 0.5×10^{21} Pa s, in agreement with the recent analyses by Lambeck *et al.* (1990), Vermeersen *et al.* (1999) and Devoti *et al.* (2001) based on postglacial rebound modeling from different perspectives, sea-level changes in the far field and long-wavelength geopotential variations. These models are chemically stratified at 420 and 670 km depth, Figure 1.3 panel (a), and the viscosity is uniform in the whole upper mantle; this stratification supports nine relaxation modes. The slowest modes have been named $M1$ and $M2$ by Wu and Peltier (1982) and are associated with the two internal chemical boundaries at 670 and 420 km. These $M1$ and $M2$ modes will be quoted several times in the book when dealing with the geophysical processes affected by the slow readjustment of the 670 and 420 km density discontinuities.

At low degrees, Figure 1.4, they are followed by the lithospheric ($L0$) mode and by the core ($C0$) and mantle ($M0$) modes, as portrayed in the panel NM by $B = 1$, with $B = \nu_2/\nu_1$ denoting the ratio between the lower to upper

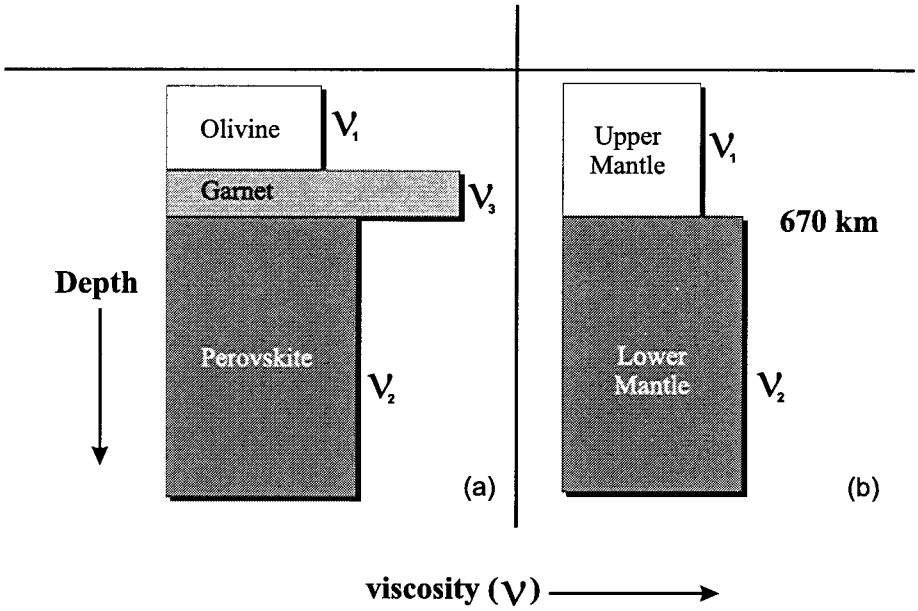

Figure 1.3. Schematic diagram with the rheological models, which include a hard transition zone, panel (a), considered for the evaluation of the relaxation times and a two-layer mantle, panel (b), shown for comparison.

mantle viscosity. When B is increased from 1 to 200, all the curves are moved upward toward slower relaxation times. This upward migration occurs first for longer wavelengths, say lower than $l = 10$, followed by the shorter ones, which are less affected by lower mantle viscosity. For shorter wavelengths only the $M1$, $M2$ and core modes have slower relaxation times, while the lithospheric and mantle modes are rather unaffected, the deformation at such high harmonic degrees being concentrated in the upper mantle and thus unaffected by lower mantle viscosity variations. The NM curves, in the left panel, can be obtained from their counterparts in the right panel by a uniform downward shift towards faster relaxation times, in agreement with the lowering of the global mantle viscosity of this model.

Figure 1.5 shows the effects of a viscosity increase in the transition zone for the new model NM, with $C = \nu_3/\nu_1$ denoting the ratio between the viscosity in the transition zone ν_3 with respect to the viscosity in the upper mantle. These models, with a stiff transition zone at the upper lower mantle boundary, are based on the laboratory studies by Karato (1989) and Meade and Jeanloz (1990), which suggest that the transition zone may form a layer of relatively high viscosity between the upper and lower mantle. The C parameter is varied between 1 and

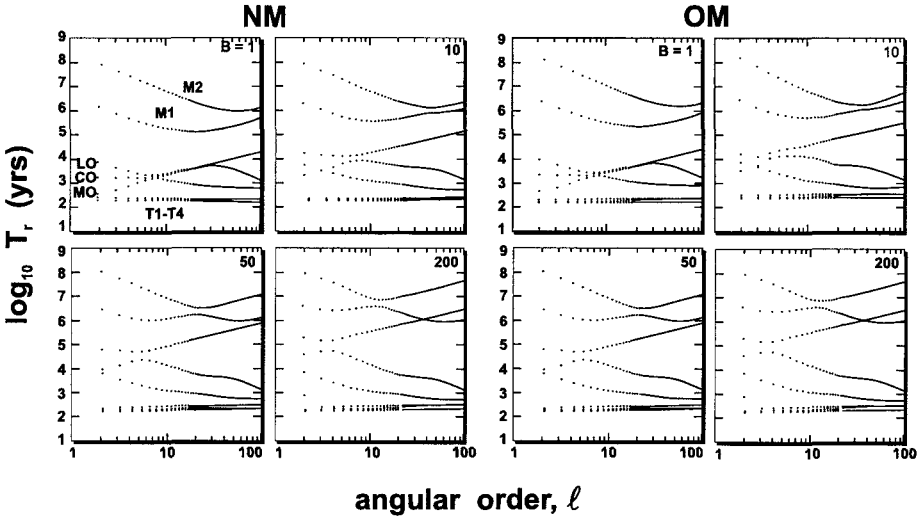

Figure 1.4. Relaxation times in years as a function of the harmonic degree l and varying lower mantle viscosity. The parameter $B = \nu_2/\nu_1$ is varied from 1 to 200. OM corresponds to $\nu_1 = 10^{21}$ Pa s, while NM corresponds to $\nu_1 = 0.5 \times 10^{21}$ Pa s. (Figure 2 in Spada *et al.*, 1992b).

200. Panel LB, with LB standing for lower bound, corresponds to an upper mantle viscosity of 0.5×10^{21} Pa s and the low value of $\nu_2 = 2 \times 10^{21}$ Pa s in the lower mantle, while UB, with UB standing for upper bound, corresponds to the same upper mantle viscosity and to a higher lower mantle viscosity of $\nu_2 = 2 \times 10^{22}$ Pa s. LB and UB for the lower mantle viscosity stand for the two possible viscosity solutions when true polar wander data and variations in the long-wavelength gravity field are used to constrain the viscosity of the lower mantle (see Chapters 4 and 5). Viscosity increase in the hard layer influences all the modes for all the models, in particular the $M1$ and $M2$ modes, which is not surprising as these modes are excited by the discontinuities that bound the region where the viscosity is varied. With respect to the previous figure, all the modes are now affected by the viscosity increase in the transition layer which, lying close to the surface, is also able to affect the short wavelength, high-degree modes.

7. PHASE-CHANGE INTERFACE

Density contrasts associated with phase changes that allow for material crossing the interface have been developed by Johnston *et al.* (1997) and applied to simplified 5-layer models. If the transition zone of the mantle behaves as a phase change, Johnston *et al.* (1997) have shown that the appropriate boundary

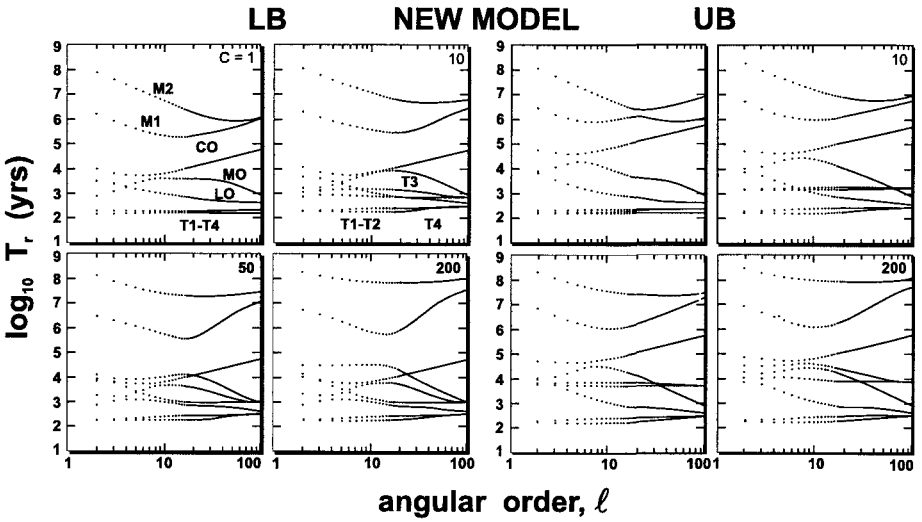

Figure 1.5. Relaxation times in years as a function of the harmonic degree l and varying lower mantle viscosity. The parameter $C = \nu_3/\nu_1$ is varied from 1 to 200. LB corresponds to $\nu_1 = 0.5 \times 10^{21}$ Pa s and $\nu_2 = 2 \times 10^{21}$ Pa s, while UB corresponds to $\nu_1 = 0.5 \times 10^{21}$ Pa s and $\nu_2 = 2 \times 10^{22}$ Pa s. (Figure 3 in Spada *et al.*, 1992b).

condition, with i, $i+1$ denoting the two layers that match at the phase-change interface, is given by

$$\mathbf{Y}^{(i)}(r_{i+1}, s)\mathbf{C}^{(i)} = (\mathbf{I} + \xi_{i+1}\boldsymbol{\alpha}_{i+1}\boldsymbol{\beta}_{i+1})\mathbf{Y}^{(i+1)}(r_{i+1}, s)\mathbf{C}^{(i+1)}, \quad (1.109)$$

where ξ_i denotes the response function for the i-th layer defined by Christensen (1985), $\mathbf{I}$ denotes the identity matrix and $\boldsymbol{\alpha}_i$, $\boldsymbol{\beta}_i$ are given by

$$\boldsymbol{\alpha}_i = (\Delta\rho_i/\rho_{i-1}, 0, 0, 0, 0, 0) \quad (1.110)$$

$$\boldsymbol{\beta}_i = (-4\mu_i/r_i, 2l(l+1)\mu_i/r_i, -1, 0, 0, 0)/(\rho_i g(r_i)), \quad (1.111)$$

where $\Delta\rho_i = \rho_{i-1} - \rho_i$ denotes the density contrast. It should be noted that the definition of $\boldsymbol{\alpha}_i$ and $\boldsymbol{\beta}_i$ differ from that given in the equation (30) by Johnston *et al.* (1997) since their procedure has been adapted to ours, where the inner layers correspond to increasing values of the index i. Equation (1.109) does not apply at rheological interfaces, like the lithosphere-mantle or core-mantle interface, where $\xi = 0$ is used.

In our propagation method, the secular equation (1.106) now becomes

$$\det\left(\mathbf{P}_1\left(\prod_{i=1}^{N-1}(\mathbf{I}+\xi_{i+1}\boldsymbol{\alpha}_{i+1}\boldsymbol{\beta}_{i+1})\mathbf{Y}^{(i)}(r_i,s)\mathbf{Y}^{(i)^{-1}}(r_{i+1},s)\right)\mathbf{I}_c(r_c)\right)=0. \tag{1.112}$$

For an univariant phase change, the response factor ξ_i takes the following explicit expression as a function of various thermodynamic parameters

$$\xi_i = 1 - \frac{\rho_i^3 g k c_p}{T w(\rho_{i+1}-\rho_i)(dP_c/dT)^2}, \tag{1.113}$$

where k is the thermal diffusivity, c_p the specific heat at constant pressure, T the absolute temperature, w the vertical component of the background convection velocity and dP_c/dT is the Clapeyron slope, which gives the rate of change of the pressure of the phase change with respect to the temperature.

Once the parameters in Table 2 of Johnston *et al.* (1997) are used, it is found that an appropriate value for the response factor at 420 and 670 km is $\xi_i = 0.7$. The physical meaning of the response factor can be easily understood if we recall here its definition in terms of the difference between the displacement ε of the interface where the phase change occurs and the particle displacement u (Johnston *et al.*, 1997).

$$\varepsilon - u(r_0) = \xi\frac{p^\delta}{\rho_{i+1}g}, \tag{1.114}$$

where p^δ is the incremental pressure due to the surface loads. If $\xi = 0$ the density contrast moves with the material particles and it denotes a chemical interface, while for $\xi = 1$ the density discontinuity due to the phase change occurs at constant pressure and is thus termed isobaric; in this case, the density jump is totally adiabatic because the temperature does not play any role in controlling the final position of the interface. Intermediate values of the response factor, in the interval between $\xi = 0$ and $\xi = 1$, are responsible for a behavior of the phase change interface between those two end members.

For an upper mantle viscosity ν_1 fixed at 10^{21} Pa s, Figure 1.6 portrays the inverse relaxation times $-1/s_i$ for variations in the lower mantle viscosity ν_2. The s_i are the zeros of the secular equations (1.106) and (1.112), top and bottom panels respectively, for the 5-layer model described in Table 2.2 where the densities are volume averages of the Preliminary Reference Earth Model (PREM) of Dziewonski and Anderson (1981).

The top panel corresponds to a chemically stratified mantle, while the bottom treats the case of a phase change with $\xi = 0.7$ at the 420 and 670 km interfaces. We notice, comparing the two panels of Figure 1.6, that the modification in the ξ parameters from 0 to 0.7 affects only the slowest buoyancy relaxation modes, as expected, with those corresponding to the phase change being slower. It is

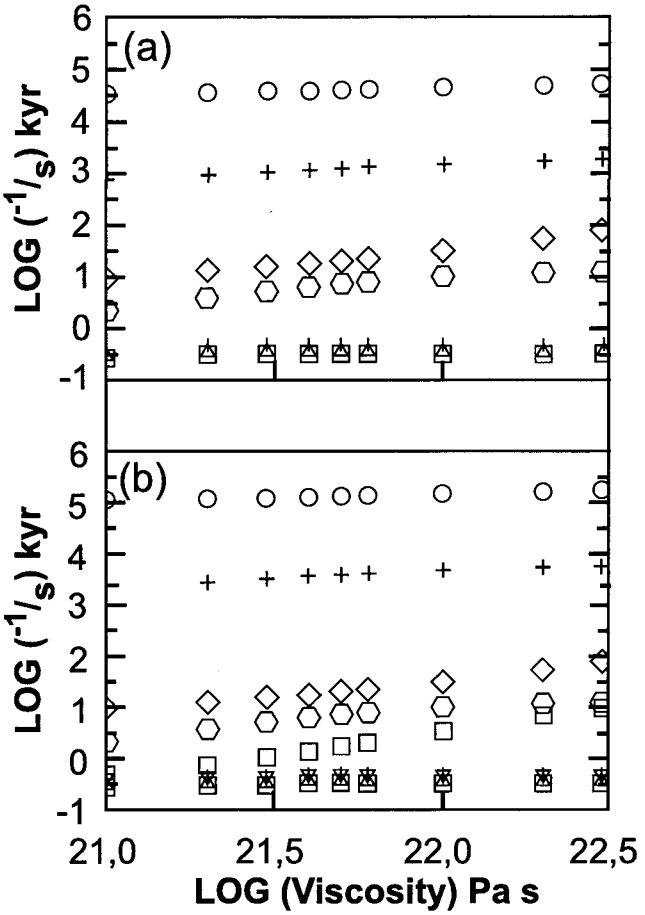

Figure 1.6. Inverse relaxation times for the isostatic modes, equations (1.106) and (1.112), for the 5-layer model of Table 2.2, for chemical and phase-change boundary conditions at 420 and 670 km, (a) and (b) panels respectively. The phase change is characterized by $\xi = 0.7$. The circles and the crosses correspond to the 420 and 670 km discontinuities. Redrawn from Figure 2 in Sabadini *et al.* (2002).

also interesting to note that these particular buoyancy modes are less sensitive to viscosity variation in the analyzed range than to changes in ξ, suggesting that the nature of the transition zone, whether chemical or phase change, must play a crucial role in the rotation dynamics of the Earth.

8. LOADING THE EARTH

The general solution of the following non-homogeneous system of ordinary differential equations for each harmonic degree l, where $\mathbf{f}$ is the vector charac-

terizing a general kind of source loading the Earth embedded at a depth r_s and $\mathbf{A}$ being the spheroidal or toroidal system matrix

$$\frac{d}{dr}\mathbf{y} = \mathbf{A}\cdot\mathbf{y} + \mathbf{f}, \tag{1.115}$$

is given by

$$\mathbf{y}(r) = \mathbf{Y}(r)[\int_{r_0}^{r} \mathbf{Y}^{-1}(r')\mathbf{f}(r')dr' + \mathbf{Y}^{-1}(r_0)\mathbf{y}(r_0)], \tag{1.116}$$

where r_0 denotes an interface lying below the source and $\mathbf{Y}(r)$ is the fundamental matrix given by equation (1.74) for the spheroidal case or equation (1.82) for the toroidal case; the harmonic degree l is not explicitly given.

In the following derivation it is assumed that the source is embedded in the outermost layer of radius a, denoting the radius of the Earth, and internal radius b, denoting the interface between the bottom of the lithosphere and underlying layer. This procedure can be generalized to a source embedded in an arbitrary internal layer. If the vector $\mathbf{f}$ has this form

$$\mathbf{f} = \mathbf{f}\delta(r - r_s), \tag{1.117}$$

with r_s denoting the radius of the source, the solution of the non-homogeneous system of ordinary differential equations takes the following form

$$\mathbf{y}(r) = \left\{ \begin{array}{ll} \mathbf{Y}(r)[\mathbf{Y}^{-1}(r_s)\mathbf{I}\,\mathbf{f} + \mathbf{Y}^{-1}(b)\mathbf{y}(b)], & r_s \le r \le a; \\ \mathbf{Y}(r)\mathbf{Y}^{-1}(b)\mathbf{y}(b), & b \le r \le r_s. \end{array} \right\} \tag{1.118}$$

Exercise. Show that, if the forcing vector has the form

$$\mathbf{f}^* = \mathbf{f}\delta(r - r_s) + \mathbf{f}'\delta'(r - r_s), \tag{1.119}$$

the solution is given by

$$\mathbf{y}(r) = \left\{ \begin{array}{ll} \mathbf{Y}(r)[\mathbf{Y}^{-1}(r_s)(\mathbf{I}\,\mathbf{f} + \mathbf{A}(r_s)\mathbf{f}') + \mathbf{Y}^{-1}(b)\mathbf{y}(b)] & r_s \le r \le a; \\ \mathbf{Y}(r)\mathbf{Y}^{-1}(b)\mathbf{y}(b), & b \le r \le r_s, \end{array} \right\} \tag{1.120}$$

where $\mathbf{A}$ is any of the matrices given by equation (1.51) or (1.81).

8.1 INTERNAL LOADING: EARTHQUAKES, SUBDUCTION

The boundary conditions for an internal forcing (earthquakes or internal density anomalies) are the vanishing of the stress components and y_6 at the Earth's surface:

$$y_3(a) = y_4(a) = y_6(a) = 0. \tag{1.121}$$

For internal density contrasts appropriate for modeling subduction processes, the $\mathbf{f}$ vector takes the form

$$\mathbf{f} = (0\ ,\ 0\ , -\frac{1}{4\pi} g(r_s)(2l+1)/{r_s}^2\ ,\ 0\ ,\ 0\ , -G(2l+1)/{r_s}^2). \tag{1.122}$$

These conditions can be cast in the following form once we make use of equations (1.119) and (1.120)

$$\mathbf{P}_1\mathbf{Y}(a)[\mathbf{Y}^{-1}(r_s)(\mathbf{If} + \mathbf{A}(r_s)\mathbf{f}') + \mathbf{Y}^{-1}(b)\mathbf{y}(b)] = 0, \tag{1.123}$$

where $\mathbf{P}_1$ denotes the projection operator on the third, fourth and sixth components of the solution vector defined in equation (1.105).

If the three-component vector $\mathbf{b}$ is defined in the following way

$$\mathbf{b} = -\mathbf{P}_1\mathbf{Y}(a)\mathbf{Y}^{-1}(r_s)(\mathbf{If} + \mathbf{A}(r_s)\mathbf{f}'), \tag{1.124}$$

the boundary conditions at the surface become

$$\mathbf{P}_1\mathbf{Y}(a)\mathbf{Y}^{-1}(b)\mathbf{y}(b)] = \mathbf{b}, \tag{1.125}$$

which coincides with equation (52) in Sabadini *et al.* (1982a).

For earthquake sources, the appropriate $\mathbf{f}$ and $\mathbf{f}'$ vectors entering equation (1.120) can be found in Appendix C.

8.2 SURFACE LOADING: POINT MASS AND TIDAL FORCING

In the case of surface loading, the loading vector $\mathbf{f}$ affects only the stress components of the solution vector and the component related to the gradient of the perturbed potential y_3, y_4, y_6. In the case of a point mass load acting at the Earth's surface, the $\mathbf{b}$ vector takes the form (Sabadini *et al.*, 1982a)

$$\mathbf{b} = (-\frac{1}{4\pi} g(a)(2l+1)/a^2\ ,\ 0\ ,\ -G(2l+1)/a^2). \tag{1.126}$$

which coincides with equation (1.122) once $r_s = a$.

For tidal forcing appropriate for solving problems related to changes in the centrifugal potential, as in the case of the Earth's rotation instabilities, the 3-component vector $\mathbf{b}$ becomes (Takeuchi *et al.*, 1962)

$$\mathbf{b} = (0\ ,\ 0\ ,\ -(2l+1)/a). \tag{1.127}$$

With these definitions, the boundary conditions at the surface for internal loading or surface loading become formally equivalent.

8.3 SOLVING FOR THE DISPLACEMENT AND PERTURBATION IN THE GRAVITATIONAL POTENTIAL

With the above definition for the $\mathbf{b}$ vector, whose expression depends on the forcing as shown previously, the boundary conditions at the Earth's surface become

$$\mathbf{b} = \mathbf{P}_1\mathbf{y}(a,s) = \mathbf{P}_1\left(\prod_{i=1}^{N-1}\mathbf{Y}^{(i)}(r_i,s)\mathbf{Y}^{(i)^{-1}}(r_{i+1},s)\right)\mathbf{I}_c(r_c)\mathbf{C}_c. \quad (1.128)$$

The unconstrained parameters U_l, V_l and ϕ_l at the surface can be expressed as

$$(U_l, V_l, -\phi_l)(a,s) = \mathbf{P}_2\mathbf{y}(a,s)$$
$$= \left(\mathbf{P}_2\prod_{i=1}^{N-1}\mathbf{Y}^{(i)}(r_i,s)\mathbf{Y}^{(i)^{-1}}(r_{i+1},s)\mathbf{I}_c(r_c)\right)\mathbf{C}_c, \quad (1.129)$$

with $\mathbf{P}_2$ as the projection operator on the first, second and fifth component of the solution vector given by

$$\mathbf{P}_2 = \begin{pmatrix} 1 & 0 & 0 & 0 & 0 & 0 \\ 0 & 1 & 0 & 0 & 0 & 0 \\ 0 & 0 & 0 & 0 & 0 & 0 \\ 0 & 0 & 0 & 0 & 0 & 0 \\ 0 & 0 & 0 & 0 & 1 & 0 \\ 0 & 0 & 0 & 0 & 0 & 0 \end{pmatrix} \quad (1.130)$$

Elimination of $\mathbf{C}_c$ from equation (1.128) and (1.129) results in

$$(U_l, V_l, -\phi_l)(a,s) = \left(\mathbf{P}_2\prod_{i=1}^{N-1}\mathbf{Y}^{(i)}(r_i,s)\mathbf{Y}^{(i)^{-1}}(r_{i+1},s)\mathbf{I}_c(r_c)\right)\cdot$$
$$\cdot\left(\mathbf{P}_1\prod_{i=1}^{N-1}\mathbf{Y}^{(i)}(r_i,s)\mathbf{Y}^{(i)^{-1}}(r_{i+1},s)\mathbf{I}_c(r_c)\right)^{-1}\cdot\mathbf{b}, \quad (1.131)$$

where $\mathbf{b}$ is any of the vectors defined in equation (1.124), (1.126) or (1.127).

Each of the M solutions s_j of equation (1.106) or (1.112) represents a singularity for the right hand member of equation (1.131). In fact, the quantity in the second brackets in the right member with

$$\mathbf{B} = \prod_{i=1}^{N-1} \mathbf{Y}^{(i)}(r_i, s)\mathbf{Y}^{(i)^{-1}}(r_{i+1}, s) \tag{1.132}$$

can be written as

$$(\mathbf{P}_1\mathbf{B}\mathbf{I}_c(r_c))^{-1} = (\mathbf{P}_1\mathbf{B}\mathbf{I}_c(r_c))^{\dagger}/\det(\mathbf{P}_1\mathbf{B}\mathbf{I}_c(r_c)), \tag{1.133}$$

where $(\mathbf{P}_1\mathbf{B}\mathbf{I}_c(r_c))^{\dagger}$ denotes the matrix of the complementary minors. The determinant $\det(\mathbf{P}_1\mathbf{B}\mathbf{I}_c(r_c))$ entering equation (1.133) can be written as $\prod_{i=1}^{M}(s - s_i)$, where the s_i are the solutions of equation (1.106) or (1.112): each s_i is thus responsible for the appearance of a singularity that corresponds to a first-order pole .

The inverse Laplace transform of equation (1.131) from the s to the time domain can thus be carried out by means of the residue theorem in Appendix B.3, as shown hereafter.

The inverse Laplace transform $f(t)$ of a function $\tilde{f}(s)$ is formally defined by complex contour integration by

$$f(t) = \frac{1}{2\pi i}\int_{\gamma-i\infty}^{\gamma+i\infty} \tilde{f}(s)e^{st}ds, \tag{1.134}$$

in which the real constant γ is chosen such that singularities of $\tilde{f}(s)e^{st}$ are either all on the left or all on the right side of the vertical line running from $\gamma - i\infty$ to $\gamma + i\infty$. Closing the contour with a half-circle (either on the left of the line or on the right, depending on where the singularities are situated) leads to a complex contour that is known as the Bromwich path.

The residue theorem states that if $\tilde{f}(s)$ is an analytical function with M singularities of first order, in our case the right hand side of equation (1.131), then

$$\frac{1}{2\pi i}\int_{\gamma-i\infty}^{\gamma+i\infty} \tilde{f}(s)e^{st}ds = \sum_{i=1}^{M}[Res(\tilde{f}(s)e^{st})]_{s=s_j}, \tag{1.135}$$

where the residue in the pole of first order $s = s_j$ is given by (equation (B.30))

$$Res(\tilde{f}(s)e^{st})|_{s=s_j} = lim_{s\to s_j}(s - s_j)\tilde{f}(s)e^{st}. \tag{1.136}$$

The above equation (1.136), with $(s - s_j)$ multiplying the function $\tilde{f}(s)$ in the s-domain and the exponential, tells us that, since at the denominator of equation (1.131) we have the product $\prod_{i=1}^{M}(s - s_i)$, we finally remain with $\prod_{i\neq j}^{M}(s_j - s_i)$ at the denominator after we have made use of it. It can be easily seen that $\prod_{i\neq j}^{M}(s_j - s_i)$ equals $\frac{d}{ds}\det(\mathbf{P}_1\mathbf{B}\mathbf{I}_c(r_c))|_{s=s_j}$.

The solution of the field U_l, V_l and $-\phi_l$ at the surface of the Earth can thus be cast in the following form of the 3-component $\mathbf{K}(t)$ vector

$$(U_l, V_l, -\phi_l)(a,t) = \mathbf{K}_l(t) = \mathbf{K}_{le}(a)\delta(t) + \sum_{j=1}^{M} \mathbf{K}_{lj}(a)e^{s_j t}, \qquad (1.137)$$

in which, on the basis of the equations above, the $\mathbf{K}_{lj}(a)$ are the vector residues of the solution kernel vector $\mathbf{y}(r,s)$ given by

$$\mathbf{K}_{lj}(a) = \left(\frac{\mathbf{P}_2\mathbf{BI}_c(r_c) \cdot (\mathbf{P}_1\mathbf{BI}_c(r_c))^\dagger}{\frac{d}{ds}\det(\mathbf{P}_1\mathbf{BI}_c(r_c))} \right)_{s=s_j} \cdot \mathbf{b}, \qquad (1.138)$$

and $\mathbf{K}_{le}(a)$ denoting the elastic limit obtained by

$$\mathbf{K}_{le}(a) = \lim_{s\to\infty} (\mathbf{P}_2\mathbf{BI}_c(r_c) \cdot (\mathbf{P}_1\mathbf{BI}_c(r_c))^{-1}) \cdot \mathbf{b}. \qquad (1.139)$$

For surface loading the dimensionless form of the first two components of the $\mathbf{K}_l$ vector are usually indicated by the Love numbers h_l, l_l for the radial and tangential displacement. The nondimensionalization constant is $\phi_{2,l}/g = a/M_E$, where $\phi_{2,l}$ is the potential perturbation due to the load and a and M_E denote rhe radius and the mass of the Earth. The third component is $\phi_{2,l}(1+k_l)$, where k_l is the Love number of the geopotential perturbation and 1 denotes the direct effect of the load.

The appearance of the delta $\delta(t)$ in the time domain is a consequence of the fact that equation (1.139) is a constant in the s-domain. These results provide the radially dependent part of the Green functions for the variables for each degree l.

Multiplying the Green functions with the Laplace-transformed forcing functions (which is the same as a convolution in the space-time domain) and performing an inverse Laplace transformation gives the sought-for expressions for the displacement fields and perturbation in the gravitational potential due to any kind of time-dependent loading.

Solution (1.137) shows that for each harmonic degree l the horizontal displacement, vertical displacement and change in gravity consist of an immediate response to the load (the elastic response), followed by M exponentially decaying (viscous) responses. At the least, the viscous responses are decaying only if the inverse relaxation times s_j for each harmonic degree are negative. For incompressible models this turns out to be always the case if the Earth layers show no density inversions in the radial Earth profile. However, if there is a layer with a greater density than its neighboring layer below, then the buoyancy mode for the interface will have a positive inverse relaxation time for each harmonic degree l. Such a positive relaxation time leads, according to equation (1.137), to an exponentially increasing response in the displacements and gravity variations, and thus the interface becomes Rayleigh-Taylor unstable. If this occurs, convective motions will be triggered in the earth model, and the

linearization assumed in the normal-mode theory as developed in this chapter breaks down.

From Chapter 3 onwards, we will make use of the superscript L in the Love numbers in order to denote a load, such as that associated with surface density anomalies, while the Love numbers corresponding to tidal loading will not carry any superscript.

9. APPROXIMATION METHOD FOR HIGH-DEGREE HARMONICS

When using spherical harmonics to describe Earth surface deformations, we always have to face the problem of how many terms we should sum up in order to obtain an accurate solution. Since every harmonic represents a standing wave on the Earth's surface, whose equator is about 40,000 km long, it is easy to determine the resolution given by each term of that series wherein the wavelength is given by the length of the equator divided by the harmonic degree. For point-like seismic sources, we find in the modeling carried out in Chapter 8 that this wavelength is uniquely related to the source depth for the elastic response and to the thickness of the elastic layer for (viscoelastic) relaxation: the summation of several thousand harmonics is thus required to get saturated convergence of the solution in the case of shallow earthquakes.

Modeling of the post-seismic effects of shallow and moderate-size earthquakes in the Mediterranean has motivated the development of new algorithms, with respect to those used for studying global post-seismic deformation as in Sabadini *et al.* (1984a) or Piersanti *et al.* (1995), appropriate for normal mode techniques at very high harmonic degrees, necessary for resolving wavelengths of a few hundred meters. These new algorithms are built on the multilayer code first developed in Vermeersen and Sabadini (1997), in which the core of the normal mode technique, namely the rootfinding procedures for multilayer models, had been modified and improved with respect to the old models (Sabadini *et al.*, 1984a; Piersanti *et al.*, 1995) in which the standard routines of rootfinding can deal with a five-layer model at the most.

The analytical propagator matrix technique, due to the stiffness of the fundamental matrices, does not allow, in practice, a straightforward calculation of more than a few thousands degrees. This is due to the $r^{\pm l}$ dependence of the fundamental matrix, equation (1.74), which causes numerical problems of over- and under-flow for high order harmonic degrees. The particular structure of the analytical fundamental solutions used in normal mode techniques thus does not allow a straightforward calculation, since numerical problems can readily occur due to the stiffness of the matrices used in the propagation routines. However, it is possible to mathematically demonstrate that the irregular fundamental solutions in non-homogeneous earth models are not necessary for calculating all the harmonic degrees, their weight getting smaller and smaller with increasing

degree. From a certain degree onwards, namely $l > 10^2 - 10^3$, depending on the earth model, it is possible to obtain an approximated expression of the fundamental solutions by keeping only the regular part. This makes it possible to remove the r^l growth of this part by rescaling procedures, as shown for the first time in Riva and Vermeersen (2002).

This section deals with a way of removing this stiffness problem by approximating the fundamental matrix solutions, followed by a rescaling procedure; in this way we can virtually go up to whatever harmonic degree is required. One way to cope with the stiffness problem is to use minors of the fundamental matrices (e.g., Woodhouse, 1988). This technique is commonly used in seismic applications that employ numerical integration by means of propagator matrices. Here we present a new alternative approximation technique that can be used for analytical propagator matrix models.

Here we will first demonstrate, by means of matrix algebra, that it is possible to obtain a first order approximation of the fundamental solutions by neglecting the irregular part of the fundamental matrix from a certain degree onwards. We will then determine the accuracy of this approximation and describe how to apply a reliable rescaling procedure. The following section is taken from Riva and Vermeersen (2002) and adapted to our formalism.

9.1 APPROXIMATION OF THE SOLUTION

Equation (1.106) for the inverse relaxation times s_j of the modes j can be changed into the following expression

$$\det[\mathbf{M}(r_1)\mathbf{B}'\mathbf{I}_c] = 0, \tag{1.140}$$

in which $\mathbf{M} = \mathbf{P}_1\mathbf{Y}^{(1)}(r_1)$ is the fundamental matrix $\mathbf{Y}$ with the first, second and fifth rows deleted (i.e., the rows corresponding to the displacements and to the gravitational potential), $\mathbf{I}_c$ is a 6×3 matrix containing the conditions at the core-mantle boundary given by equation (1.103) and $\mathbf{B}'$ differs from equation (1.132) and is given by

$$\mathbf{B}' = {\mathbf{Y}^{(1)}}^{-1}(r_2) \prod_{i=2}^{N-1} \mathbf{Y}^{(i)}(r_i){\mathbf{Y}^{(i)}}^{-1}(r_{i+1}). \tag{1.141}$$

With these definitions, the residues, i.e. the amplitudes of the modes j, for each of the roots s_j are thus given by

$$\mathbf{K}_{lj} = \left(\frac{\mathbf{N}(r_1)\mathbf{B}'\mathbf{I}_c \cdot [\mathbf{M}(r_1)\mathbf{B}'\mathbf{I}_c]^\dagger}{\frac{d}{ds}\det[\mathbf{M}(r_1)\mathbf{B}'\mathbf{I}_c]} \right)_{s=s_j} \cdot \mathbf{b}, \tag{1.142}$$

where the vector $\mathbf{b}$ is defined in section 1.8.2 for surface loading, $\mathbf{N}$ is $\mathbf{Y}^{(1)}(r_1)$ with the third, fourth and sixth rows deleted (corresponding to the stresses and the potential gradient) and the † symbol denotes the $(-1)^{i+j}$-transposed of the nine minor determinants of the matrix between the brackets, with i and j denoting the number of rows and columns. The elastic response is given as the limit for s going to infinity of the same relation (1.142), without the $s-$derivative.

We now focus on the incompressible case; explicit expressions for $\mathbf{Y}$ for the compressible case can be found in Appendix A.

The problem we have to deal with in calculating residuals given by equation (1.142) is that the fundamental matrix $\mathbf{Y}$ contains three regular functions r^l and three irregular r^{-l}. The radii are non-dimensionalized by division by the average Earth radius a and are thus represented by a number between zero and one; it is obvious that

$$\lim_{l\to\infty} r^l \longrightarrow 0 \quad \text{and} \quad \lim_{l\to\infty} r^{-l} \longrightarrow +\infty. \tag{1.143}$$

Especially for deep layers ($r \simeq 1/2$ at the CMB), and due to the stiffness of the matrices, numerical evaluation of the fundamental solutions can represent a serious problem for high-degree harmonics; for practical purposes, then, we need to find a way to rescale equations (1.140) and (1.142). However, the propagation matrix technique, which is at the basis of the explicit form for $\mathbf{B}'$ (or $\mathbf{B}$ in equation (1.132)), does not allow a simple rescaling due to the non-commutativity of the matrix algebra. The fundamental matrix is stiff and this stiffness, in turn, would require rescaling by means of a transformation like $\mathbf{Y}' = K\mathbf{Y}$, with K being a 6×6 linear operator. But once we put all the $\mathbf{Y}'$ and $(\mathbf{Y}')^{-1}$ into (1.140) and (1.142) we have no way, at the end of the calculations, to find an inverse transformation which can produce the actual values for the relaxation times and their residuals.

The explicit analytical form of the layer propagator matrix $\mathbf{Y}\mathbf{Y}^{-1}$ can be found in Martinec and Wolf (1998); note, however, that use of the explicit analytical form of the propagator matrix in the propagator matrix technique does not solve the stiffness problem.

However, there is an approximation method that does solve the stiffness problem, as discussed in the following section.

The basic idea underlying the approximation procedure is to consider the 6×6 matrix $\mathbf{Y}$ as formed by two 6×3 matrices, one regular ($\mathbf{Y}_R$) and one irregular ($\mathbf{Y}_I$),

$$\mathbf{Y} = [\, \mathbf{Y}_R \;\; \mathbf{Y}_I \,]. \tag{1.144}$$

This splitting can also be found in Sabadini *et al.* (1982a). The first three rows of the inverse $\mathbf{Y}^{-1}$ can be cast as a 3×6 irregular matrix that we define as $\mathbf{Y}_U^{-1}$.

We then split $\mathbf{B}'$ into two parts as well, $\mathbf{B}_U$ (up) and $\mathbf{B}_D$ (down), both 3×6,

$$\mathbf{B}' = \begin{bmatrix} \mathbf{B}_U \\ \mathbf{B}_D \end{bmatrix}, \tag{1.145}$$

and we will demonstrate below that $\mathbf{B}_U$ is irregular and $\mathbf{B}_D$ regular. The matrix $\mathbf{N}$ of equation (1.142) is evaluated at the surface and keeps the same structure as $\mathbf{Y}$ (left part regular, right irregular), so that performing the products in equation (1.142) results in

$$\mathbf{N}\mathbf{B}'\mathbf{I}_c = [\,\mathbf{N}_R\ \mathbf{N}_I\,] \begin{bmatrix} \mathbf{B}_U \\ \mathbf{B}_D \end{bmatrix} \mathbf{I}_c = \mathbf{N}_R\mathbf{B}_U\mathbf{I}_c + \mathbf{N}_I\mathbf{B}_D\mathbf{I}_c. \tag{1.146}$$

In this way we have separated $\mathbf{N}\mathbf{B}'\mathbf{I}_c$ into the two terms $\mathbf{N}_R\mathbf{B}_U\mathbf{I}_c$ and $\mathbf{N}_I\mathbf{B}_D\mathbf{I}_c$, which present a different behavior since

$$\lim_{l\to\infty} \mathbf{N}_R\mathbf{B}_U\mathbf{I}_c \longrightarrow +\infty, \quad \text{whereas} \quad \lim_{l\to\infty} \mathbf{N}_I\mathbf{B}_D\mathbf{I}_c \longrightarrow 0. \tag{1.147}$$

The same holds for $\mathbf{M}\mathbf{B}'\mathbf{I}_c$ in equation (1.142) and we are thus allowed to write

$$\lim_{l\to\infty} \mathbf{N}\mathbf{B}\mathbf{I}_c \longrightarrow \mathbf{N}_R\mathbf{B}_U\mathbf{I}_c \quad \text{and} \quad \lim_{l\to\infty} \mathbf{M}\mathbf{B}\mathbf{I}_c \longrightarrow \mathbf{M}_R\mathbf{B}_U\mathbf{I}_c. \tag{1.148}$$

As a result, when we determine the products in equation (1.142) by taking into account equation (1.148), we obtain

$$\lim_{l\to\infty} \mathbf{K}_{lj} \longrightarrow \left(\frac{\mathbf{N}_R\mathbf{B}_U\mathbf{I}_c \cdot (\mathbf{M}_R\mathbf{B}_U\mathbf{I}_c)^\dagger}{\frac{d}{ds}\det(\mathbf{M}_R\mathbf{B}_U\mathbf{I}_c)} \right)_{s=s_j} \cdot \mathbf{b}. \tag{1.149}$$

The relaxation times result from the approximated form of the secular equation (1.140):

$$\det[\mathbf{M}_R\mathbf{B}_U\mathbf{I}_c] = 0, \tag{1.150}$$

with $\mathbf{B}_U$ defined as

$$\mathbf{B}_U = \mathbf{Y}^{(1)}{}_U^{-1}(r_2) \prod_{i=2}^{N-1} \mathbf{Y}^{(i)}{}_R(r_i)\mathbf{Y}^{(i)}{}_U^{-1}(r_{i+1}). \tag{1.151}$$

We can demonstrate that $\mathbf{B}'$ keeps the same structure as in equation (1.145) (upper part irregular, lower part regular) independently of the number of layers. It is possible to rewrite equation (1.141) by grouping the matrices evaluated at the same radii and by isolating the one at the CMB:

$$\mathbf{B}' = \left[\prod_{i=2}^{N-1} \mathbf{Y}^{(i-1)^{-1}}(r_i)\mathbf{Y}^{(i)}(r_i)\right] \mathbf{Y}^{(N-1)^{-1}}(r_c). \tag{1.152}$$

It is evident, then, that all couples of matrices evaluated at the same radii compensate each r_i^l term with an analogous r_i^{-l} term: the only net dependence on the radius is from the inverse fundamental matrix at the CMB. As a consequence, the general structure of $\mathbf{B}'$ is the same as $\mathbf{Y}^{-1}(r_c)$, thus characterized by an irregular upper part and a regular lower one (as is clear from the structure of the fundamental matrix and from $\mathbf{Y}\mathbf{Y}^{-1} = \mathbf{I}$).

A further refinement of this last result is also possible. A direct consequence of equation (1.152) is the possibility of applying only a partial approximation to equation (1.141), instead of the full one in equation (1.151), by splitting the product into two parts:

$$\prod_{i=2}^{NA-1} \mathbf{Y}^{(i-1)^{-1}}(r_i)\,\mathbf{Y}^{(i)}(r_i) \prod_{i=NA}^{N-1} \mathbf{Y}_U^{(i-1)^{-1}}(r_i)\,\mathbf{Y}_R^{(i)}(r_i), \tag{1.153}$$

where NA is the first boundary where approximated solutions are used. In this way a good compromise can be found between approximation accuracy and numerical stability. As a general rule, the resolution required by shallow seismic events can be reached by approximating boundaries only within the lower mantle, typically represented by the CMB itself.

The possibility of a partial approximation becomes crucial to implementing the case of an internal mantle loading as a pointlike seismic source in the crust or lithosphere: these applications will be shown in Chapter 8, dealing with post-seismic deformation.

All the arguments presented continue to hold and no further demonstration is required when the approximation is applied below the source: the new terms only consist of matrices evaluated at the surface and at the source depth and are thus not affected by the approximation.

9.2 RESCALING THE SOLUTION

As anticipated above, the net dependence of the amplitudes on the basis functions in the $\mathbf{B}'$ matrix results from the inverse fundamental matrix evaluated at the CMB.

Considering that only the first column of $\mathbf{I}_c$ depends on powers of the radius (see equation (1.103)), due to the free-slip boundary condition at the interface with the fluid core, it is easy to show that

$$\mathbf{N}_R\mathbf{B}_U\mathbf{I}_c \cdot (\mathbf{M}_R\mathbf{B}_U\mathbf{I}_c)^\dagger \,(:) \begin{bmatrix} r_c^{-2l} & r_c^{-2l} & r_c^{-2l} \\ r_c^{-2l} & r_c^{-2l} & r_c^{-2l} \\ r_c^{-2l} & r_c^{-2l} & r_c^{-2l} \end{bmatrix} \tag{1.154}$$

and

$$\det(\mathbf{M}_R\mathbf{B}_U\mathbf{I}_c)\,(:)\, r_c^{-2l} \tag{1.155}$$

so that, once we make use of equations (1.154) and (1.155) to evaluate equation (1.149), the dependence on r_c^{-2l} compensates between the numerator and the denominator.

The key point consists in the possibility of taking the $r^{\pm l}$ dependence out of the computation at the very beginning and to obtain the same residues. This can be done by normalizing $\mathbf{Y}_R$ by means of r^l and $\mathbf{Y}_U^{-1}$ by means of r^{-l}. In this way the stiffness problem is avoided.

The accuracy of the approximation is analyzed for the value of elastic and fluid Love numbers for an incompressible Earth in the case of surface loading. All the results are expressed as normalized residuals

$$k_{norm.res.} = \left| \frac{k - k_{app.}}{k} \right|, \tag{1.156}$$

with k the Love number without the approximation and $k_{app.}$ the approximated Love number. In the figures, a square represents the radial displacement number, a triangle the tangential displacement and a circle the gravitational ones.

The earth model taken into consideration is characterized by five layers: an elastic lithosphere 120 km thick, a viscoelastic mantle with chemical discontinuities at 420 km and 660 km and, finally, an inviscid core. Values for rigidity and density are PREM-averaged (Dziewonski and Anderson, 1981) as in Table 2.2 of the following chapter and viscosity in the mantle is fixed at 10^{21} Pa s.

In Figure 1.7 we show the elastic k normalized residues of the Earth when the approximation procedure is started at different depths. In panel (a) we take the regular part of the solution only at the core-mantle boundary: differences between exact and approximated Love numbers are up to 40% but affect only the first few terms and are negligible for degree 10 and higher. In panel (b) we rescale all the boundaries from the 420 km discontinuity downwards (i.e. also at 660 km and the CMB): the vertical and gravitational responses are highly affected (more than 100% difference) but still converge quite rapidly to the exact solution (1% difference at degree 50); the horizontal Love number is

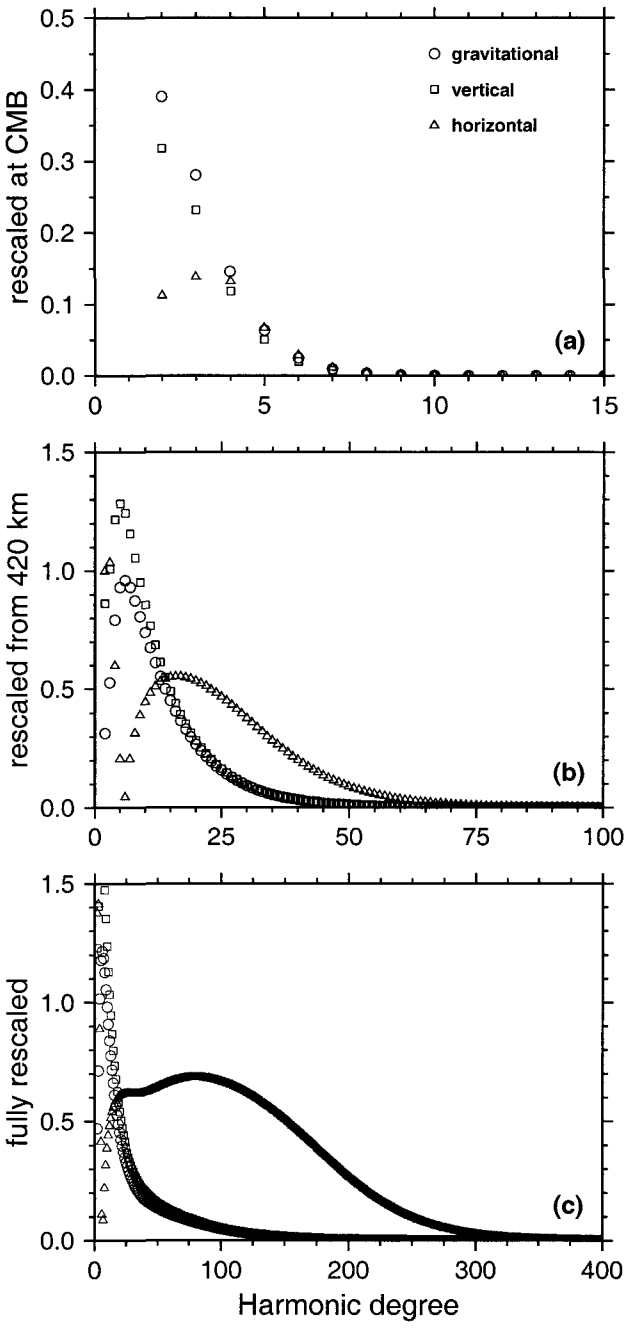

Figure 1.7. Normalized residual elastic Love numbers (Figure 1 in Riva and Vermeersen, 2002).

less affected, but convergence is slower (less than 1% at degree 70). Finally, in panel (c), full approximation is applied: more terms are required before reaching convergence between the exact and the approximated solution (1% difference around degree 160 for the vertical and the gravitational numbers), in particular for the horizontal Love number which remains significantly different for the first 200 terms and reaches the 1% level around degree 330.

In Figure 1.8 we show the effect of the approximation for the fluid response: results are not significantly different from the elastic case. When only the CMB is approximated, as in panel (a), convergence is very fast and the maximum difference is limited (only the gravitational number is above 10% for degree 2). When approximation is started at 420 km, as in panel (b), both vertical and gravitational Love numbers show a discrepancy from the exact solution smaller than 20% and again a fast convergence (below 1% at degree 25), whereas a few more horizontal terms are highly affected. This last feature, however, is due to the fact that the horizontal fluid number is changing sign around degree 10 and the normalization is not appropriate. The only limit we found is the impossibility of applying the approximation at a boundary with an elastic layer when the fluid response is evaluated: null residuals are obtained in this case. This fact, however, does not represent a real problem, since several thousand terms are already reached by just rescaling the solution at deeper boundaries. Another important issue is the numerical computation of spherical harmonics using the recursive relation for the Legendre polynomials: results up to degree 60,000 have been compared after working with both double- and quadruple-precision and the relation appears to be stable. The stiffness problem can thus be overcome by applying a successful approximation and rescaling procedure to the analytical propagator matrix technique commonly employed in normal mode models. The irregular fundamental solutions in non-homogeneous earth models can be neglected, the weight getting smaller and smaller with increasing harmonic degree. Keeping only the regular part of the fundamental solution makes it possible to by-pass the non-commutativity problem of the matrix algebra and to rescale the solution within the propagation procedure. Thus, the method presented here is an alternative to the minors-only method commonly employed in (seismic) numerical normal mode modeling.

These results provide a quantitative estimate of the applicability of the approximation procedure. In practice, in most cases it is only necessary to rescale the CMB, which means that just the first few terms need the full solution in order to obtain adequate results. However, even when the solution is fully approximated, good results are obtained after a few hundred terms.

This approach has been explicitly discussed for the case of an incompressible linear rheology due to the availability of a short explicit form for both the fundamental matrix and its inverse. This assumption is not necessary for the

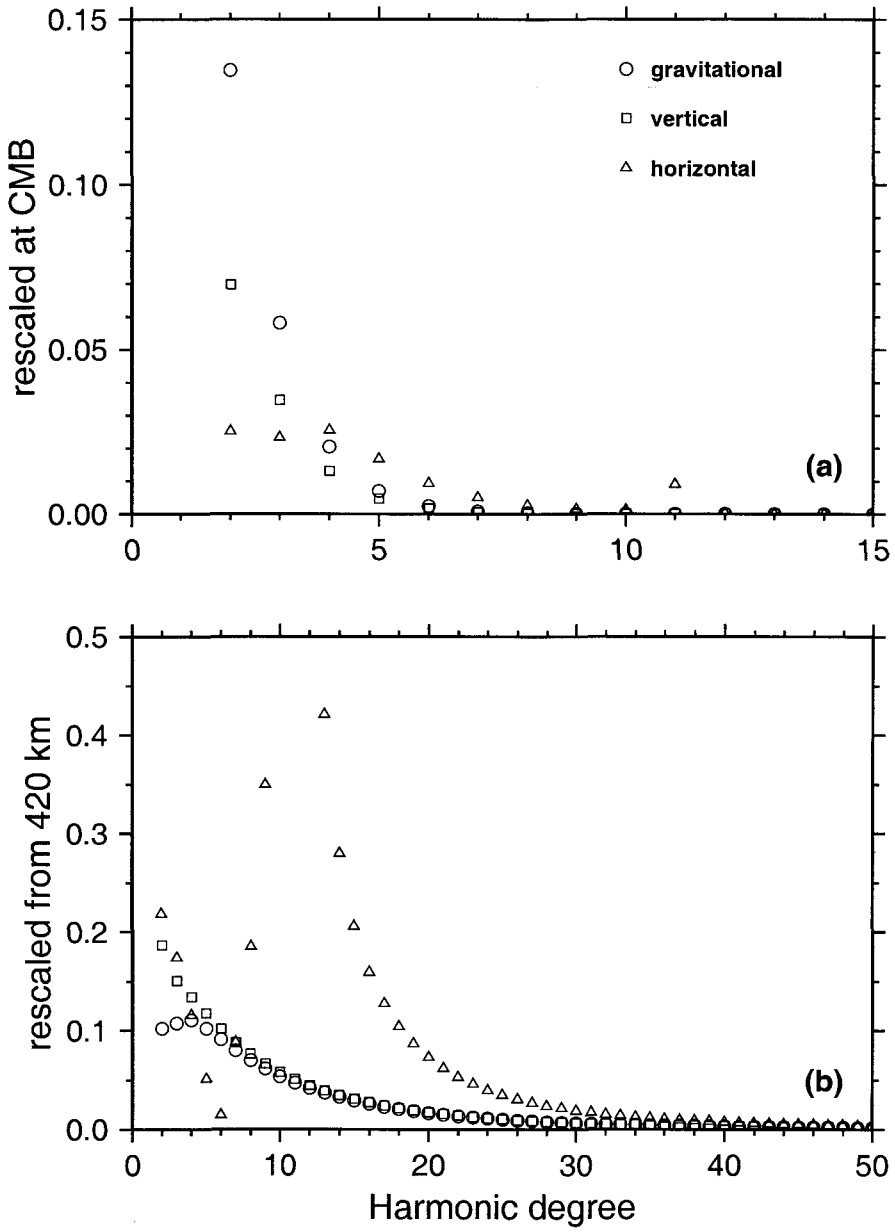

Figure 1.8. Normalized residual fluid Love numbers (Figure 2 in Riva and Vermeersen, 2002).

demonstration, as the character of the fundamental solutions (regular/irregular) is the only information which is required.